Collision-free motions of round robots on metric graphs

Marjan Safi Samghabadi

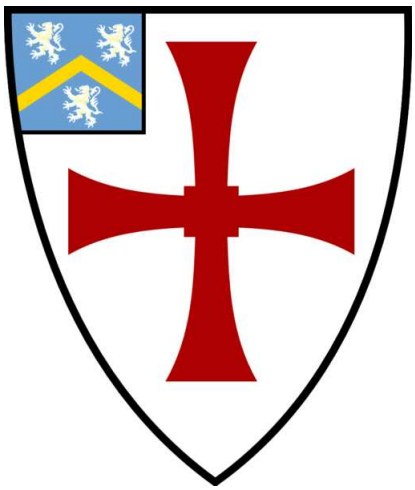

A thesis presented for the degree of
Doctor of Philosophy

Pure Mathematics
Department of Mathematical Sciences
Durham University

2013

Abstract

Collision-free motions of round robots on metric graphs

Marjan Safi Samghabadi

In this thesis, we study the path-connectivity problem of configuration spaces of two robots that move without collisions on a connected metric graph. The robots are modelled as metric balls of positive radii. In other words, we wish to find the number of path-connected components of such a configuration space. Finding a solution to this problem will help us to understand which configurations can be reached from any chosen configuration.

In order to solve the above problem, we show that any collision-free motion of two robots can be replaced by a finite sequence of elementary motions. As a corollary, we reduce the path-connectivity problem for a 2-dimensional configuration space to the same problem for a simple 1-dimensional subgraph (the configuration skeleton) of the space.

Declaration

The work in this thesis is based on research carried out in the Pure Mathematics Group at the Department of Mathematical Sciences, Durham University. No part of this thesis has been submitted elsewhere for any other degree or qualification and it is all my own work unless referenced to the contrary in the text.

Acknowledgements

I would like to thank my parents Maryam and Abdollah and my brother Mohammad for all their love and support which eneabled me to come to Durham to study.
It is my immense gratitude that I thank the support and help of my supervisor Dr Vitaliy Kurlin. He was very generous with his time and supporting me with my studies.

I am grateful for the support from Dr Theresa McKinven and Mrs Brenda Ryder from Ustinov college and Mrs Emma Foster from DSU. Also I would like to thank Dr Olaf Post for spending time on proof checking my thesis. I consider it an honor to have met and have discussions with Dr Vernon Armitage, Dr John Bolton, Dr Joan Camps, Dr Buddhapriya Chakrabarti, Dr Peter Craig, Prof Patrick Dorey, Dr Chih-hao Fu, Prof Ruth Gregory, Dr Ostap Hryniv, Dr Cherry Kearton, Dr Andrew Lobb, Dr Dirk Schuetz, Prof David Wooff and Prof Wojtek Zakrzewski.
It was my good fortune to have made friends with Anne Atkinson, Camila Caiado, Kenneth Deeley, Thomas Dessain, Samaneh Javan, Sedigheh Mirzaii, Pamela Kelly, Foad Lotfifar, John Mcleod, Sepehr Meshkinfamfard, Benedict Powell and Ramón Vera. I also wish to thank my cousin, Saeid Mehri Yari for having good discussions about topics related to my research.
Those I wish to thank who helped and encouraged me before I came to Durham are: Miss Gohar Ansari, Mr Gholam Hossein Arab, Mrs Shayesteh Biyok, Mrs Fatemeh Eslami, Mrs Khorgamfar, Dr Ehsan Momtahan, Mrs Nayeri, Mrs Ashrafsadat Shekarbaghani and Dr Mostafa Zebarjad.

Last but not least, I wish to dedicate this thesis to Dr Sharry Borgan as without his support it would not have been possible for me to have completed it.

Notation

$\chi(G)$: The Euler characteristic of G.

$OC(G,n)$: The **o**rdered **c**onfiguration space of n zero-sized robots on the connected graph G.

$UC(G,n)$: The **u**nordered **c**onfiguration space of n zero-sized robots on the connected graph G.

$OD(G,n)$: The **o**rdered **d**iscrete configuration space of n zero-sized robots on the connected graph G.

S_n: The symmetric group S_n is the group of all permutations on n symbols.

$OC(G,n;r_1,r_2,\ldots,r_n)$: The **o**rdered **c**onfiguration space of n robots with the radii r_1, $r_2 \ldots$, r_n on the connected metric graph G.

$SP(a,b)$: The set of all non-self intersecting shortest paths between the points a, b on the connected metric graph G.

$EC(G,2;r_1,r_2)$: The number of all isolated **e**xtreme **c**onfigurations plus the number of connected components of closures of punctured circles in the set of all extreme configurations.

$CS(G,2;r_1,r_2)$: The **c**onfiguration **s**keleton of 2 robots with radii r_1, r_2 on the connected metric graph G.

Contents

Chapter 1

Introduction

In this thesis, we are interested in the collision-free motions of two robots on a connected metric graph. We will define the space of all configurations of two robots on a connected metric graph when the two robots do not collide. So we do not allow configurations where the two robots are too close to each other. Therefore, the space of all collision-free configurations may have several components. The main result of this thesis is an algorithm that computes the number of components in the space of all collision-free motions of two robots on a connected metric graph. This algorithm can be used in the control system of robot motions. At this point, it is interesting to have an overview about the the history of Artificial Intelligence. In the following section, we will review the initial ideas of Artificial Intelligence and how it developed to its current place.

1.1 History

The idea of building an intelligent machinery began in ancient days, by investigating the possibilities of "placing mind into matter," or " machinizing formal reasoning" [29]. In the 12th century, the problem was described as a machine which combines basic truths by simple logical operations and produces all knowledge [29]. This investigation evolved in the 1600's, by exploring the possibilities of formulating all rational thoughts. In the 20th century, it has been proved that it is possible to machinize the formulated knowledge, though it is not possible to express all thoughts by Mathematical reasoning [29]. Finally, in 1956, in the Dartmouth Conference, the academic field of *Artificial Intelligence* was

born leading to many significant developments; mainly improved efficiency and precision in manufacturing, service and healthcare industries [29].
This intelligent machine was called *robot* after Joseph Capek used the term to describe the automates in his fiction story *Opilec* in 1917 [30]. The first industrial robot, *Unimate* was used on the assembly line in 1961, and since then robots have been applied in deep sea, space exploration, military use and for search and rescue missions [17]. In 1992, robots called *Robodoc* have been used in hip replacement surgeries. Robots are classified into two groups of *active* and *passive*, where the former is programmable and the latter translates movements from an operator.
Due to the extension and variety of applications of robots in daily life, the research carried out in robotics is significantly increasing every year [17]. Among the many different challenges arising in the field of Artificial Intelligence, there are some questions which can be solved using mathematical tools.

In this thesis, we are interested in the problems that are classified as *computational topology* in the field of Mathematics. Computational topology applies the tools such as homology, knot theory, dynamical systems, topological robotics and Morse theory etc., to solve applied problems like Hierarchical clustering, denoising density functions, shape description, surface reconstruction, robot arm motion planning, robot motion planning and algorithmic problems [32]. More precisely, we are interested in applying topological tools to solve problems that are applied in robotics, for example, it is possible to describe the configuration spaces of robots which are moving on a magnetic tape on the factory floor, by using Euler characteristic, homology groups, and homotopy theory e.t.c. The resulting information about configuration spaces will help us to understand the motion of robots. In the following section, we will review research that has been performed in the area of configuration spaces.

1.2 Background

In this section, we have a brief overview of the past research related to topological robotics. The problem of finding different topological invariants of the topological space, so called

configuration space is the main motivation of most research carried out in this topic. Traditionally, robots follow a guide-path of magnetic tapes on the factory floor. This tradition naturally leads to modelling the problem of studying the motion of robots on graphs. Many interesting results when the number of robots is limited to 2 have been achieved in considerably short period of time. The simplified model when robots are points have been mostly studied by R. Ghrist [13], D. Koditschek [12], J. Swiatkowski [27]. Further progress achieved by K. Barnett and M. Farber in [3], and has been generalised by M. Farber and E. Hanbury in [9]. A generalised case has been studied by A. Abrams, D. Gay and V. Hower; in [2]. The generalised problem for the finite number of points on trees was studied by M. Farber [7]. The configuration spaces of robots on trees have also been studied by D. Farley and L. Sabalka [10]. Braid groups of configuration spaces have been studied by V. Kurlin [20]. Research related to braid groups have been done by P. Prue and T. Scrimshaw [24], M. Doig and F. connolly [5], Neels and S. Privitera [23]. The most recent result on configuration spaces of finite number of robots on graphs has been provided by Ki Hyoung Ko and Hyo Won Park [19]. The model has been modified to configuration spaces of 2 metric balls on metric graphs by K. Deeley in [6]. In line with K. Deeley's research, this thesis explores solutions to the generalised question of when there are 2 metric balls of different radii on metric graphs. In the following section, the plan of this thesis will be described.

1.3 Thesis plan

This thesis investigates the path-connectivity problem for configuration spaces of robots defined as metric balls on graphs.

In Chapter 1, first we will review a brief summary of how and why we study these types of problems, then we explain the link between the giant field of Artificial Intelligence and the problems covered by this thesis, by introducing the young research area of computational topology. Finally, we list a number of studies on the problems related to this thesis.

In Chapter 2, we will review basic definitions that we need to know to continue reading the following chapters. In section 2.1, we explain the model when two robots are zero-sized. We define the space of configurations for two zero-sized robots on a graph. Then we define the discrete configuration as a subspace of configuration space. In section 2.2, we consider the model when robots are metric balls and review the background of configuration spaces of two robots on a metric graph.

In Chapter 3, we investigate the possibility of solving the path-connectivity problem by reducing the configuration space to a small set of extreme configurations. In this chapter, we will discover that extreme configurations play a vital role in connectivity of the configuration space.

In Chapter 4, we look at the initial problem "how to find number of path-connected components of the configuration space of two robots on a metric graph" with fresh eyes, and construct the configuration skeleton, for which the number of path-connected components can be computed easily. In this chapter, we begin with the definition of a subgraph for the configuration space and several examples to explain the definition. We claim such subgraph contains the same number of path-connected components as the configuration space. In Theorem 4.13, we will explain the main technique in details. Finally, we state the main result in Corollary 4.16.

Chapter 2

Configuration spaces of graphs

2.1 Topological configuration spaces

Definition 2.1. A *combinatorial graph* G consists of a finite set $V(G)$ of vertices and a finite set $E(G)$ of unoriented edges. Each edge has two vertices at its endpoints. A *loop* is an edge whose endpoints coincide. The *degree* of a vertex v is the number of edges with the endpoint v, where any loop at v is counted twice. A *hanging vertex* is a vertex of degree one. A *cycle* is a sequence of distinct edges that starts and finishes at the same vertex. A *tree* is a connected graph without cycles.

Definition 2.2. We will define the *natural topology* on a combinatorial graph G with $V(G)$ vertices. We draw any $V(G)$ points on $\mathbb{R}^2$. For any edge $\{u,v\}$ of the graph G, we draw an arc between the corresponding points on $\mathbb{R}^2$. If needed, we will slightly deform all arcs to make sure that any two arcs intersect only at double crossings. We resolve each crossing by pushing one of its arcs in $\mathbb{R}^3$. In the resulting subset $G \subset \mathbb{R}^3$, edges meet only at vertices, so G has the subspace topology of $\mathbb{R}^3$.

Definition 2.3. The *Euler characteristic* $\chi(G)$ of a topological graph G with a finite set $V(G)$ of vertices and a finite set $E(G)$ of edges is defined as $\chi(G) = V(G) - E(G)$.

Lemma 2.4. *A connected topological graph G with $V(G)$ vertices and $E(G)$ edges is homotopy equivalent to a wedge of $1-\chi(G) = 1+E(G)-V(G)$ circles.*

Proof. We can contract edges (not loops) of G one by one until we get a wedge of $l(G)$ circles with a single vertex. Since the Euler characteristic $\chi(G) = V(G) - E(G)$ is

presented under these elementary homotopy equivalence, then

$$V(G) - E(G) = \chi(G) = 1 - l(G).$$

□

Definition 2.5. A *zero-sized robot* is a point on the connected graph G.

In the following Definition we define the space of all collision-free motions of zero-sized robots on the connected graph G called the configuration space.

Definition 2.6. The *ordered topological configuration space* of n zero-sized robots on a connected graph G is

$$OC(G,n) = \{(x_1,\ldots,x_n) \in G^n \mid x_i \neq x_j \text{ if } i \neq j\}.$$

The symmetric group S_n acts on $OC(G,n)$ by permuting n robots. The quotient space $UC(G,n) = OC(G,n)/S_n$ is called the *unordered configuration space* of n zero-sized robots on G.

$OC(G,n)$ is an $n-$dimensional complicated space. Our aim is to understand the topology type of the space $OC(G,n)$, or at least the homotopy type of $OC(G,n)$. We are mainly interested in path-connectedness of $OC(G,n)$, because any two configurations in a path-connected component of $OC(G,n)$ are connected by a collision-free motion.

Definition 2.7. [22] Given points x and y of a topological space X, a *path* in X from x to y is a continuous map $f : [0,1] \to X$ such that $f(0) = x$ and $f(1) = y$. A space X is said to be *path-connected* if every pair of points of X can be joined by a path in X.

Example 2.8. Consider two zero-sized robots on the segment $[0,1]$ as shown in Fig. 2.1. The configuration space $OC([0,1],2)$ is the set of all pairs (x,y) where $0 \leq x \leq 1$, $0 \leq y \leq 1$, $x \neq y$. The line $x = y$ in the square is dashed, because the robots can not be at the same point in $[0,1]$. The configuration space $OC([0,1],2)$ is a union of two triangles and has the homotopy type of two single configurations $(0,1)$, $(1,0)$. Similarly, $OC([0,1],n)$ has the homotopy type of $n!$ disjoint points.

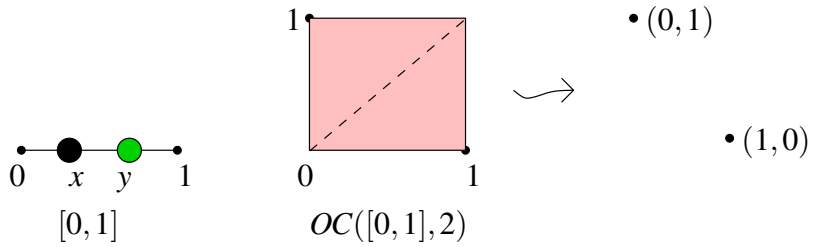

Figure 2.1: $OC([0,1],2)$ is a union of two triangles. See Example 2.8.

Example 2.9. Consider two zero-sized robots on a circle S^1 as shown in Fig. 2.2. Then $OC(S^1,2) = \{(x,y) \in S^1 \times S^1 \text{ such that } x \neq y\}$. This is a torus without the circle $x = y$. As shown in Fig. 2.2, we represent the torus as the quotient of a square and remove the circle $x = y$. After a cut-and-paste surgery in Fig. 2.2 we have an annulus without its boundary. The configuration space $OC(S^1,2)$ is homeomorphic to an open annulus which deformation retracts to a circle. Therefore, $OC(S^1,2)$ is path-connected.

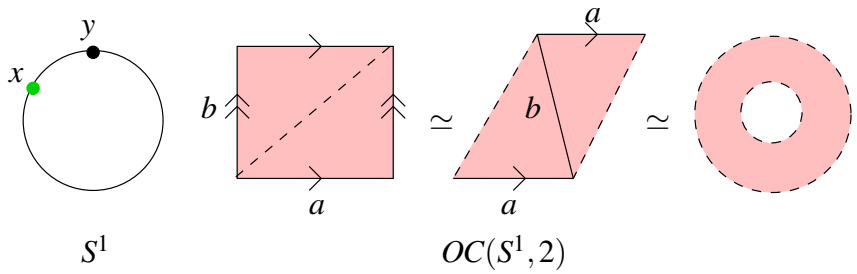

Figure 2.2: $OC(S^1,2)$ is homeomorphic to an annulus. See Example 2.9.

Example 2.10. If we have three zero-sized robots, we move them to the points $a = 0$, $b = \frac{2\pi}{3}$, $c = \frac{4\pi}{3}$ on the circle. The robots can move continuously from the configuration (a,b,c) to (c,a,b). But it is not possible for the robots to move continuously from (a,b,c) to (a,c,b) as shown in Fig. 2.3. Therefore, $OC(S^1,3)$ consists of two path-connected components. Similarly, for n zero-sized robots on a circle, the configuration space $OC(S^1,n)$ has $(n-1)!$ path-connected components.

In the following example, we explain how to swap n robots on a graph with at least one vertex of degree greater than 2.

Example 2.11. Consider three zero-sized robots on a tripod. By moving two robots to an edge and moving the third robot to the edge without robots, the robots can swap after few such steps as shown in Fig. 2.4.

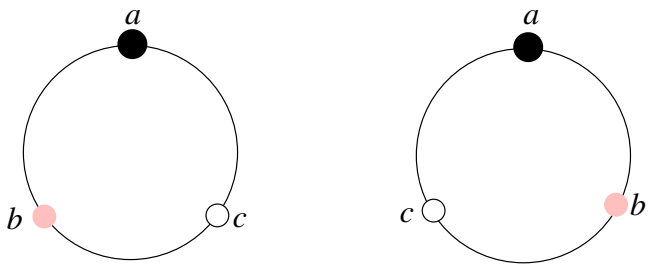

Figure 2.3: (a,b,c), (a,c,b) are not in the same path-connected component of $OC(S^1,3)$. See Example 2.10.

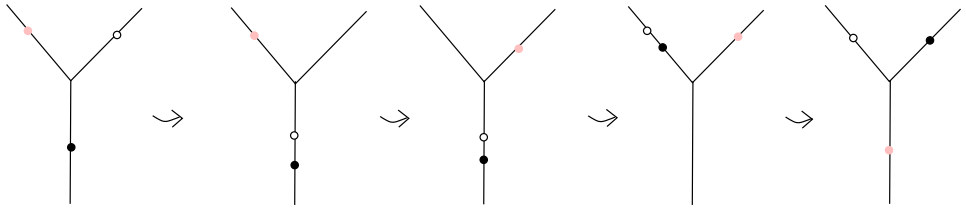

Figure 2.4: Robots can swap without collision on the tripod. See Example 2.11.

Lemma 2.12. *For a connected graph G not homeomorphic to S^1, the space $OC(G,n)$ is path-connected if and only if G contains a vertex of degree at least* 3.

If the graph G does not contain any vertex of degree at least 3, the graph G is either a circle or a segment. As we have seen in Example 2.8, the configuration space $OC(G,2)$ is not path-connected. In the exceptional case when G is homeomorphic to a circle, $OC(S^1,n)$ for $n > 2$ robots is not path-connected as shown in Example 2.10.

Example 2.13. Consider two zero-sized robots on the tripod as shown in Fig. 2.5. In this example we have two cases. (1) When both zero-sized robots are on the same edge. This is the same as Example 2.8. (2) When two zero-sized robots are on different edges. Then we can construct $OC(T_3,2)$ by identifying sides of six triangles and six rectangles produced in cases (1), (2), respectively. The configuration space $OC(T_3,2)$ is shown in Fig. 2.5. For more details about this example see [15, Section 3].

Proposition 2.14. *[13] If a connected graph G has m vertices of degree greater than* 2, *and $n > m$ then the $n-$dimensional configuration space $OC(G,n)$ deformation retracts to an $m-$dimensional cell complex.*

When the connected graph has one vertex, i.e. $m = 1$ in Proposition 2.14, we will have the following Corollary.

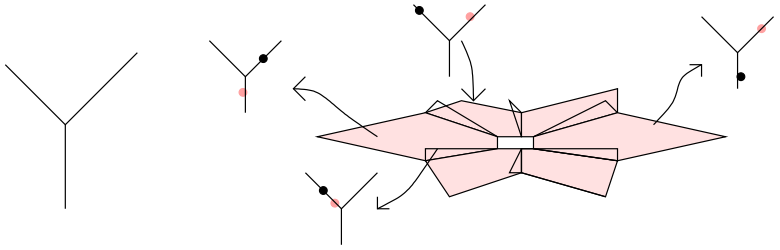

Figure 2.5: $OC(T_3,2)$. See Example 2.13.

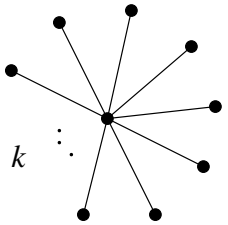

Figure 2.6: The graph T_k.

Corollary 2.15. *[15] For $k \geq 2$ graph T_k in Fig. 2.6, the space $OC(T_k,n)$ has the homotopy type of a wedge of Q circles, where*

$$Q = 1 + \frac{(n+k-2)!}{(k-1)!}(k(n-1)-2n+1).$$

By substituting $k = 3$, $n = 2$, we get $Q = 1$. This computation agrees with Example 2.5 when the configuration space $OC(T,2)$ deformation retracts to a circle.

Corollary 2.16. *For the wedge $T_{k,l}$ of $k \geq 2$ segments and l circles in Fig. 2.7, the space $OC(T_{k,l},n)$ has the homotopy type of a wedge of Q circles, where*

$$Q = 1 + \frac{(k+l+n-2)!}{(k+l-1)!}(k(n-1)+l(2n-1)-2n+1).$$

Proof. The configuration space $OC(T_{k,l},n)$ has the homotopy type of a graph by Proposition 2.14 and deformation retracts to a wedge of $1-\chi(OC(T_{k,l},n))$ circles by Lemma 2.4.

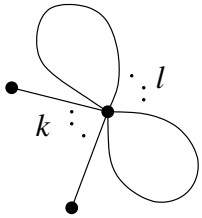

Figure 2.7: The graph $T_{k,l}$.

In [8, Section 2.1] all Euler characteristic $\chi(OC(G,n))$ are combined in the power series

$$\mathfrak{eu}_G(t) = \sum_{n=0}^{\infty} \chi(OC(G,n)) \frac{t^n}{n!}.$$

The power series $\mathfrak{eu}_G(t)$ is presented explicitly in [8, Theorem 2.6]. For the graph $T_{k,l}$ we compute $\mathfrak{eu}_{T_{k,l}}(t)$ as follows.

$$\begin{aligned}\mathfrak{eu}_{T_{k,l}}(t) &= (1-t)^{-(k+l)} \cdot (1+(1-k-2l)t) \\ &= \left[1+\cdots+\binom{k+l+n-2}{n-1}t^{n-1}+\binom{k+l+n-1}{n}t^n+\ldots\right]\cdot(1+(1-k-2l)t).\end{aligned}$$

expanding the brackets, the only two terms with t^n are

$$\binom{k+l+n-1}{n}+\binom{k+l+n-2}{n-1}(1-k-2l) = \frac{\chi(OC(T_{k,l},n))}{n!}. \quad \square$$

The 2-dimensional configuration space of two robots on $T_{1,1}$ is homotopically equivalent to a wedge of three circles, since $k=1$, $l=1$, then $Q=3$.

Example 2.17. Consider the graph K_5. The configuration space $OC(K_5,2)$ deformation retracts to a 2-dimensional surface of genus 6. See the details in [1, Example 5.1]. In [1, Example 5.2], the graph G is $K_{3,3}$. The configuration space $OC(K_{3,3},2)$ deformation retracts to a 2-dimensional surface of genus 4.

Example 2.18. Consider two robots on the graph $T_{1,1}$. By Corollary 2.16, we expect the configuration space $OC(T_{1,1},2)$ deformation retracts to a wedge of three circles. The cell structure shown in Fig. 2.8 illustrates the configuration space $OC(T_{1,1},2)$.

Example 2.19. Consider two robots on the graph $T_{0,2}$. By Corollary 2.16, we expect the configuration space $OC(T_{0,2},2)$ deformation retracts to a wedge of seven circles. The cell structure shown in Fig. 2.9 illustrates the configuration space $OC(T_{0,2},2)$.

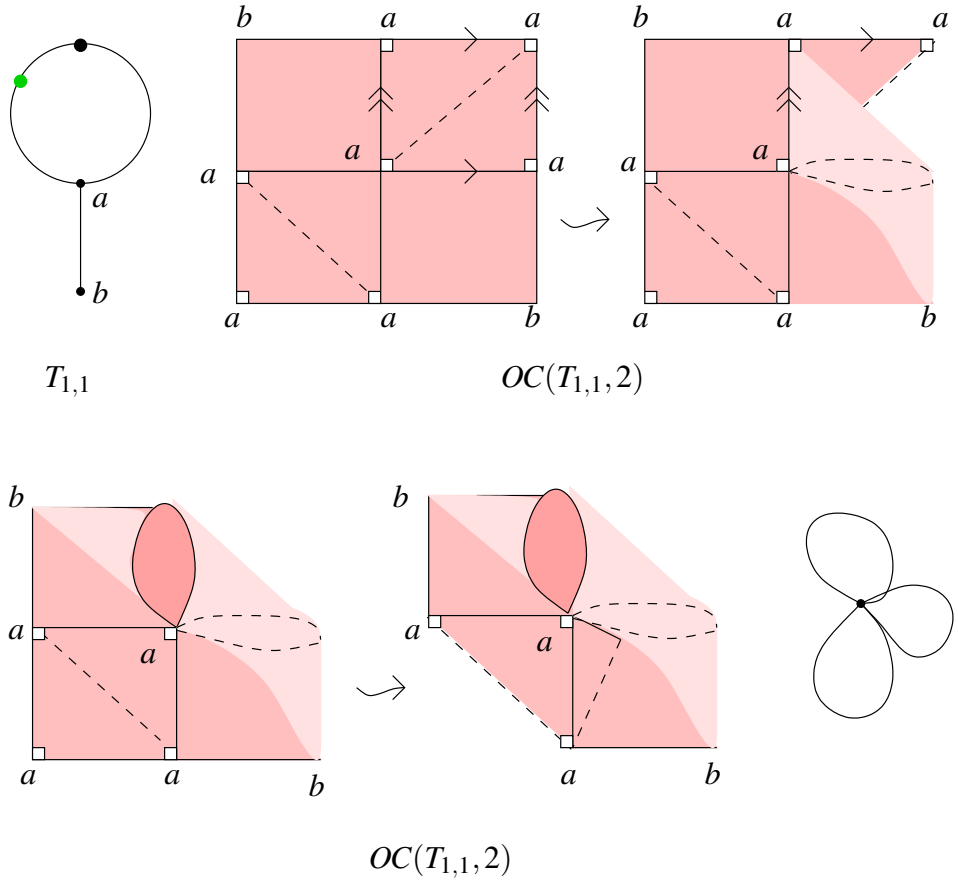

Figure 2.8: $OC(T_{1,1},2)$. See Example 2.18.

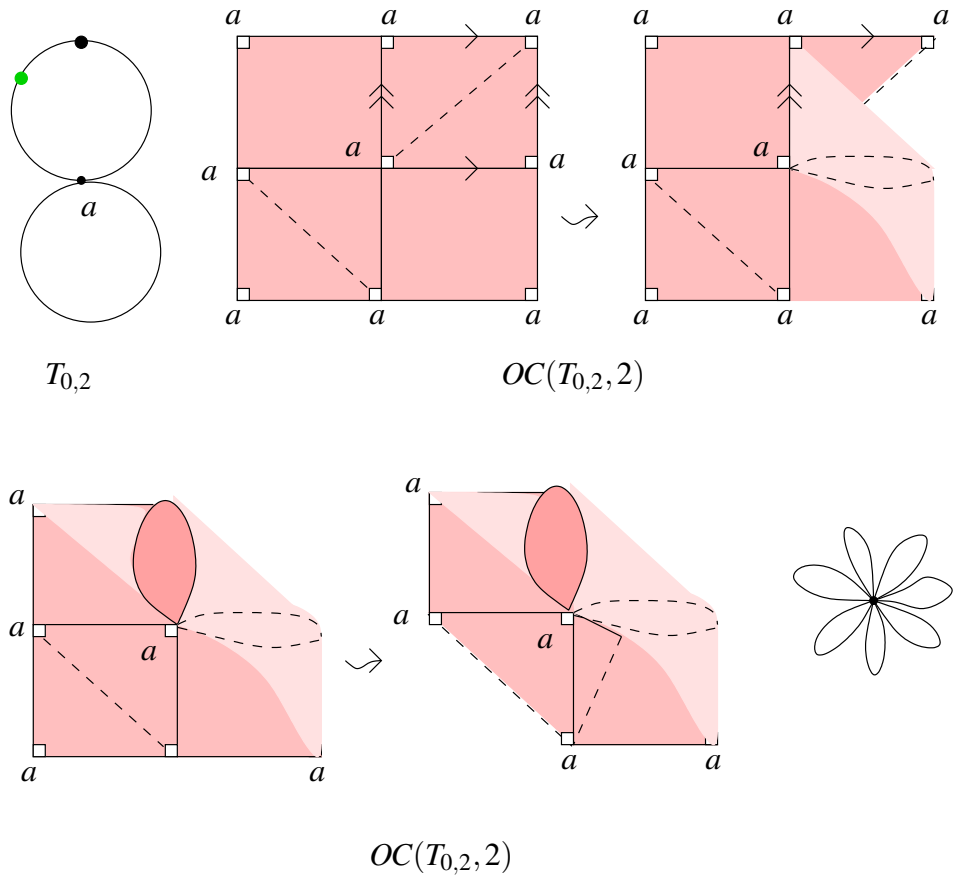

$T_{0,2}$ $OC(T_{0,2},2)$

$OC(T_{0,2},2)$

Figure 2.9: $OC(T_{0,2},2)$. See Example 2.19.

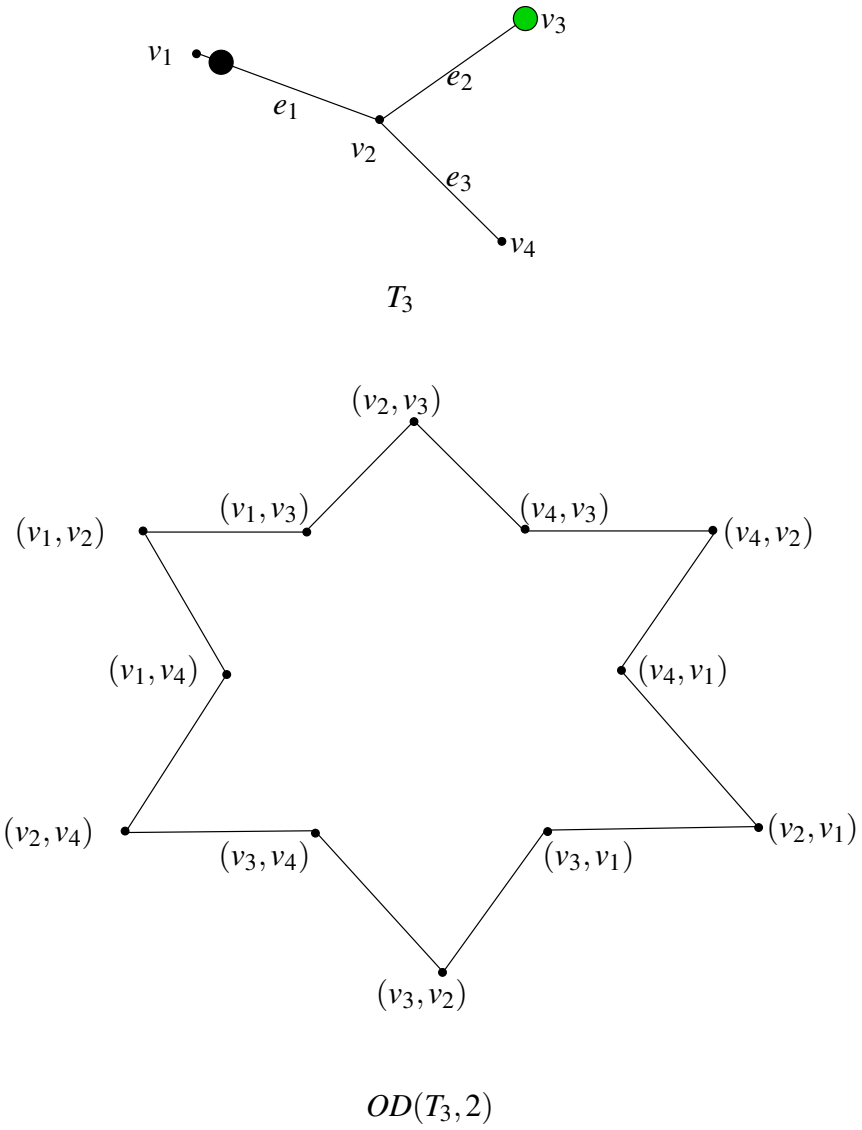

Figure 2.10: Discrete configuration space $OD(T_3,2)$.

Definition 2.20. The *discrete configuration space OD(G,n)* is a closed subspace of $OC(G,n)$ such that any two robots are at least one edge away from each other on the graph G.

Example 2.21. Consider two robots on the graph T_3 as shown in Fig. 2.10. In order to find the discrete configuration $OD(T_3,2)$, we fix first robot at vertex v_1 and move the next robot along closed edges e_2, e_3. If first robot moves along e_1, then second robot should stay either at v_3 or v_4. The space of such motions is shown as $OD(T_3,2)$ in Fig. 2.10.

2.2 Configuration spaces of robots on metric graphs

Definition 2.22. To introduce a metric graph, we start from a combinatorial graph G and fix a length $l(e) \in \mathbb{R}^+$ for any edge $e \in E(G)$. So we assume that each edge e is isometric to the segment $[0, l(e)]$ in the Euclidean line. Then the distance $d(x,y)$ between any two points x, $y \in G$ is the length of a shortest path between x, y. The distance function $d(x,y)$ makes G a *metric graph*.

Definition 2.23. We define a *robot* x in a metric graph G as a metric ball with a radius $r \in \mathbb{R}^+$ and a centre at a point $x \in G$. The distance between two robots is the distance between their centres. In other words, robot x is the set of points $y \in G$ such that $d(x,y) \leq r$.

Example 2.24. If the centre of a robot is a hanging vertex x of G, then the metric ball centred at x is the closed arc of length r, not $2r$. Two robots x, y with a radius $r > 0$ are geometrically shown by thick lines on the connected graph H in Fig 2.11. Let all edges have the same length. Therefore, there are two shortest paths of the same length from x to y, via e_2 or e_3.

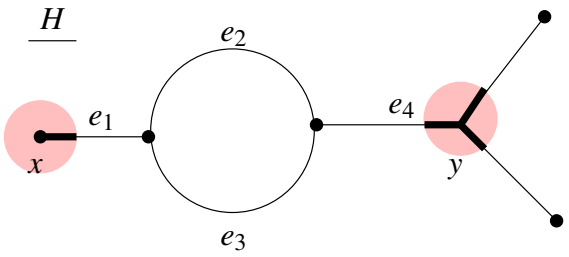

Figure 2.11: There are two shortest paths via e_2 or e_3 between x, y.

Example 2.25. Consider graph G with 5 edges as shown in Fig. 2.12. The length of the edges are π, 2π and 2. The robot x with radius π is shown with the thick lines.

Example 2.26. The robot x with radius 3 is shown with thick lines on the connected metric graph G in Fig. 2.13. The robot x consists of all the points y on the graph G when $d(x,y) \leq 3$.

Definition 2.27. The configuration space $OC(G,n;r_1,r_2,\ldots,r_n)$ of n robots with radii $r_i > 0$ for $i = 1,\ldots,n$, on a connected metric graph G, consists of all configurations of robots $(x_1,\ldots,x_n) \in G^n$ such that $d(x_i,x_j) \geq r_i + r_j$ for $i,j \in \{1,\ldots,n\}$, $i \neq j$.

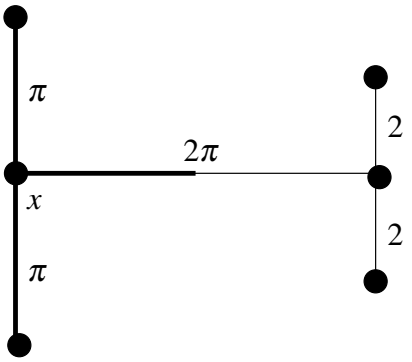

Figure 2.12: See Example 2.25.

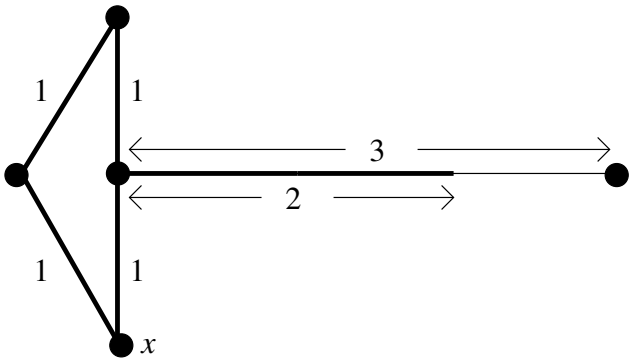

G

Figure 2.13: See Example 2.26.

Following the definition above, the configuration space $OC(G,n;r_1,r_2,\ldots,r_n)$ is compact, since we allow robots to touch each other when $d(x_i,x_j) = r_i + r_j$. So we exclude the limit case when all $r_i = 0$ because the inequalities $d(x_i,x_j) \geq 0$ allow collisions of zero-sized robots.

Example 2.28. As we considered in Section 2.1, the configuration space $OC(G,n)$ is not path-connected if G not homeomorphic to a circle, does not contain any vertices of degree greater than 2. Moreover, for $n = 2$ the connected graph G, if $l(e) > 3r$ for every edge, then two robots can swap without touching each other. Precisely, *two robots can sit on any edge* and all edges have at least the capacity of one and a half robots. Putting this together with having a vertex of degree greater than 2, the graph G has at least three edges which can hold two robots and it is easy to see two robots can permute on G, as shown in Fig. 2.14.

Proposition 2.29. *[6] If a connected metric graph G contains at least one vertex of degree*

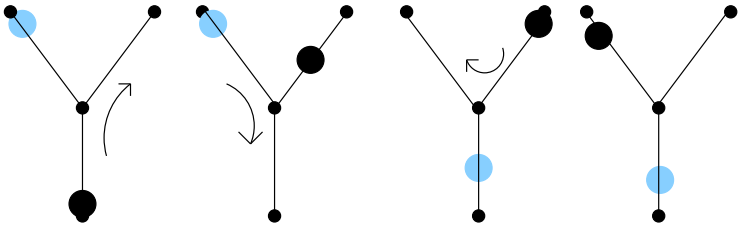

Figure 2.14: from left to right, swapping black robot with the gray robot.

greater than 2 *and* $r(2n-1) < l(e)$ *for all* $e \in E(G)$*, then* $OC(G,n;r)$ *is path-connected.*

Proof. In this case, $OC(G,n;r)$ is homotopically equivalent to $OC(G,n)$, the ordered configuration space of n zero-sized robots on G. Since G contains a vertex of degree greater than 2, it is possible to rearrange robots very similar to the case shown in Fig. 2.14. Therefore, $OC(G,n;r)$ is path-connected.

□

Lemma 2.30. *Every path-connected component of* $OC(G,n;r_1,r_2,\ldots,r_n)$ *is compact.*

Proof. The graph $G \subset \mathbb{R}^3$ and the space $OC(G,n;r_1,r_2,\ldots,r_n)$ is a closed and bounded subspace of $\mathbb{R}^{3n}$. Therefore, $OC(G,n;r_1,r_2,\ldots,r_n)$ is compact. □

Example 2.31. Consider two robots of radii r_1, r_2 on the graph $G = [0,1]$. When $r_1 = r_2 = \frac{1}{2}$, the configuration space $OC([0,1],2;\frac{1}{2},\frac{1}{2})$ consists of two isolated configurations $(0,1)$, $(1,0)$. When r_1, $r_2 \leq \frac{1}{2}$, the configuration space $OC(G,2;r_1,r_2)$ consists of two symmetric triangles as shown in Fig. 2.15 (right). When $r_1 + r_2 > 1$, the configuration space $OC(G,2;r_1,r_2)$ is empty. All configurations (x,y) are in $OC(G,2;r_1,r_2)$ satisfy the condition of Definition 2.27 as $|x-y| \geq r_1 + r_2$.

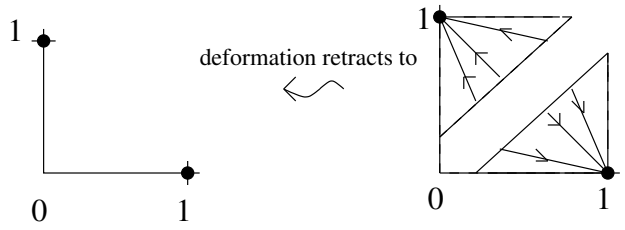

Figure 2.15: $OC([0,1],2;r_1,r_2)$. See Example 2.31.

Lemma 2.32. *Let* l *be the length of the shortest edge of a connected metric graph* G*. If* $0 < r_1 < r_2 < \frac{1}{2}l$*, then* $OC(G,2) \simeq OC(G,2;r_1,r_2)$.

Proof. In [6], has been shown that $OC(G,2) \simeq OC(G,2;r_1,r_2)$, where robots have equal radii. In this argument robots have different but sufficiently small radii, so that

$r_1 < r_2 \leq r < \frac{1}{2}l$. □

2.3 Problems

Definition 2.33. The *Euler characteristic* $\chi(G)$ of a topological graph G with a finite set $V(G)$ of vertices and a finite set $E(G)$ of edges is defined as $\chi(G) = V(G) - E(G)$.

Any connected graph G is homotopy equivalent to a wedge of $n = 1 - \chi(G)$ circles and has the free fundamental group of rank n.

Definition 2.34. [22]Let the point x belong to the space X. The set of path homotopy classes of loops based at x equipped with the operation $*$ defined by

$$f * g(s) = \begin{cases} f(2s), & 0 \leq s \leq \frac{1}{2} \\ g(2s-1), & \frac{1}{2} \leq s \leq 1 \end{cases}$$

is called the *fundamental group* of X relative to the *base point* x and is denoted by $\pi_1(X,x)$.

Definition 2.35. [18, Section 1.1]The *braid group* B_n is the group generated by $n-1$ generators $\sigma_1, \sigma_2, \ldots, \sigma_{n-1}$ and the *braid relation*

$$\sigma_i \sigma_j = \sigma_j \sigma_i$$

for all $i, j = 1, 2, \ldots, n-1$ with $|i-j| \geq 2$, and

$$\sigma_i \sigma_{i+1} \sigma_i = \sigma_{i+1} \sigma_i \sigma_{i+1}$$

for $i = 1, 2, \ldots, n-2$. The kernel of the natural projection $f : B_n \to S_n$ is called the *pure braid group* P_n.

Lemma 2.36. *[1, Section 3.2] If G is a tree, then the fundamental group of* $OC(G,2)$ *is free.*

The fundamental group of the ordered configuration space $OC(G,n)$ is also called the *pure braid group* $P_n(G)$ of n strands on the graph G. The fundamental group of the unordered configuration space $UC(G,n)$ is called *braid group* and is denoted by $B_n(G)$.

Example 2.37. If all edges of K_5 have length 1 and $r_1 < r_2 < \frac{1}{2}$, then the fundamental group of $OC(K_5,2;r_1,r_2)$ is not free.

Indeed, by Lemma 2.32, we have $OC(K_5,2;r_1,r_2) \simeq OC(K_5,2)$. By Example 5.1 in [1, Section 5.1], $OC(K_5,2)$ deformation retracts to the closed orientable surface of genus 6. Therefore, fundamental group $\pi_1(OC(K_5,2)) = \pi_1(OC(K_5,2;r_1,r_2))$ is not free.

We conclude that, for a connected metric graph G, the configuration space $OC(G,2;r_1,r_2)$ might not be homotopy equivalent to a graph.

For instance, $OC(K_5,2;r_1,r_2)$ is not homotopy equivalent to a graph, so we can not construct a graph that has the same homotopy type as $OC(K_5,2;r_1,r_2)$. Similarly, for a connected metric graph, the configuration spaces $OC(G,n;r_1,r_2,\ldots,r_n)$ led to the new wide class of "braid" groups $\pi_1(OC(G,n;r_1,r_2,\ldots,r_n))$.

Chapter 3

Extreme configurations of robots

In this chapter, we consider two robots moving on a connected metric graph G. Then we define an special type of configurations called extreme configurations. At an extreme configuration, any slight perturbation of two robots reduces the distance between them. We shall show that there are finitely many isolated extreme configurations. In the following section we formally define an extreme configuration, and prove that any configuration can be moved to an extreme configuration.

3.1 Moving a configuration to an extreme one

At any time, two robots can be anywhere on a connected metric graph G as far as they do not collide with each other. Considering they move away from each other, we explore those situations when the distance between two robots can not be increased.

Definition 3.1. For a connected metric graph G, a configuration $(a,b) \in OC(G,2;r_1,r_2)$ is called an *extreme* configuration if $d(a,b) \geq d(x,y)$, for all $(x,y) \in U_a \times U_b$, where U_a, U_b are sufficiently small open neighbourhoods of a, b, respectively. Such a configuration is called an *isolated* extreme configuration if $d(a,b) > d(x,y)$, where $(x,y) \neq (a,b)$, for any $(x,y) \in V_a \times V_b$, for sufficiently small open neighbourhoods V_a, V_b.

Example 3.2. If $0 < r_1 + r_2 \leq 1$, the pairs $(0,1)$, $(1,0) \in OC([0,1],2;r_1,r_2)$ are isolated extreme configurations since the robots are at the furthest distance from each other as shown in Fig. 3.1. If $0 < r_1 + r_2 \leq 1$, any diametrically opposite pair on the circle is a non-isolated extreme configuration in $OC(S^1,2;r_1,r_2)$ as shown in Fig. 3.2.

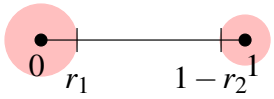

Figure 3.1: The isolated extreme configuration $(0,1)$. See Example 3.2.

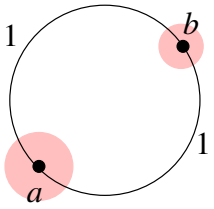

Figure 3.2: The non-isolated extreme configuration (a,b). See Example 3.2.

So two robots can move from any configuration of a path-connected component of $OC(G,2;r_1,r_2)$ to an extreme configuration in the same path-connected component. By the following result, the path-connectivity problem for $OC(G,2;r_1,r_2)$ is reduced to the smaller subset of all extreme configurations. The diameter of a graph G denoted by $\mathrm{diam}(G)$ is the length of the longest non-self-intersecting path in G.

Proposition 3.3. *There is at least one extreme configuration in any path-connected component of* $OC(G,2;r_1,r_2)$ *for* $0 < r_1 + r_2 \leq diam(G)$.

Proof. If $(x,y) \in OC(G,2;r_1,r_2)$ is not extreme, by Definition 3.1 there exist $a \in U_x$ and $b \in U_y$ such that $d(a,b) > d(x,y)$. We can push two robots away from each other until they reach an extreme configuration. Indeed, since the distance between two robots x, y is $d(x,y) \geq r_1 + r_2$, the configuration space $OC(G,2;r_1,r_2)$ is compact. □

The following definition will be used in Definition 3.6 to define a type of extreme configurations in $OC(G,2,r_1,r_2)$.

Definition 3.4. For any points a, $b \in G$, let $SP(a,b)$ be the set of all shortest non-self-intersecting paths between a, b.

Example 3.5. In Fig. 3.2, the set $SP(a,b)$ consists of two symmetric semi-circles with the endpoints a, b. In Fig. 3.1, there is a unique path between two robots.

We have seen in Definition 3.1 that at extreme configurations, the robots are locally at the furthest distance. Now, we will define a new type of configuration.

Definition 3.6. Points a, $b \in G$ are called *antipodal* if both the following conditions hold:
1) the set $SP(a,b)$ contains at least two different paths;
2) all edges at a, b belong to the paths from $SP(a,b)$.

Example 3.7. For the graph shown in Fig. 3.3, we have the set $SP(a,c) = \{abc, adbc, adc\}$. Since each edge at a and c belongs to a path in $SP(a,c)$, we can say a, c are antipodal. In Fig. 3.4, there are three paths from a to b. One path has length three, while two paths have length two. So the path with length three does not belong to $SP(a,b)$. Therefore, a, b are not antipodal.

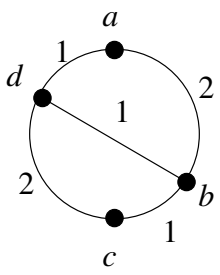

Figure 3.3: $SP(a,c) = \{abc, adbc, adc\}$, so a, c are antipodal points. See Example 3.7.

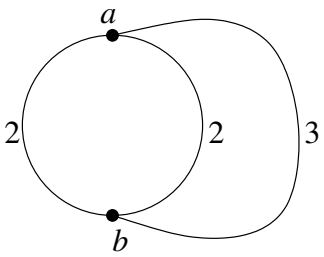

Figure 3.4: a, b are not antipodal.

Remind that a topological circle is a subgraph homeomorphic to S^1 and a hanging vertex is a vertex of degree one. All possible cases of antipodal points are described in the following lemma.

Lemma 3.8. *If a, b are antipodal points then exactly one of the following cases is true.*
(1) *The points a, b are hanging vertices; see Fig. 3.5*(1).
(2) *The point a is a hanging vertex and b is on a topological circle (or vice versa); see Fig. 3.5*(2).
(3) *The points a, b are non-hanging vertices not on the same topological circle; see*

Fig. 3.5(3).

(4) *The points a, b are diametrically opposite points on the same circle; see Fig. 3.5*(4).

Proof. If a is not on any topological circle, then all shortest paths from a to b should start with the same edge at a, otherwise, the union of two paths starting with different edges at a contains a topological circle. Then by Definition 3.6, the point a has only one edge, and we arrive at one of the cases (1) or (2). If a, b are not hanging, by Definition 3.6, then we can either have case (3) or case (4). If a, b are antipodal points on the same circle, then a, b are diametrically opposite. □

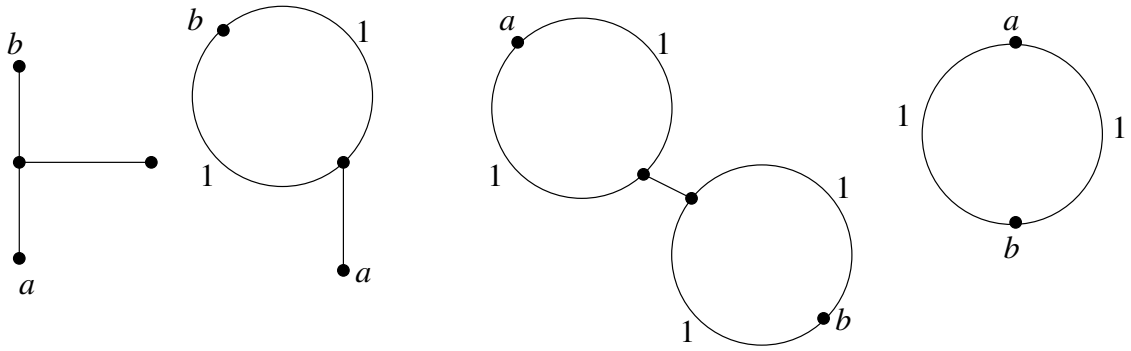

Figure 3.5: All four cases of antipodal points, see Lemma 3.8.

3.2 A characterisation of extreme configurations

We investigate for which two points a, b of a graph, (a,b) is an extreme configuration. When we consider a configuration (a,b) from the space $OC(G,2;r_1,r_2)$, we always assume that $d(a,b) \geq r_1 + r_2$ without stating explicitly further.

Lemma 3.9. *If a, b are hanging vertices of a metric graph G and $d(a,b) \geq r_1 + r_2$, then (a,b) is an isolated extreme configuration in $OC(G,2;r_1,r_2)$.*

Proof. Since $\deg a = 1$, then any shortest path from a to another vertex can become only shorter if a is slightly perturbed. (Similarly for b). □

Lemma 3.10. *If a, b are non-hanging antipodal points of a connected metric graph G and $d(a,b) \geq r_1 + r_2$, then (a,b) is an extreme configuration in the space $OC(G,2;r_1,r_2)$.*

Proof. We shall prove that (a,b) satisfies Definition 3.1. Namely, if x, y are sufficiently close to a, b, then $d(a,b) \geq d(x,y)$. Since a, b are antipodal, then by Definition 3.6, all edges at a, b belong to the shortest paths between a, b, and there are at least two such paths.

- **Case 1.** If x, y are on the same shortest path between a, b, then $d(x,y) < d(a,b)$ as shown in Fig. 3.6.
- **Case 2.** If x, y are on different paths, then for $\Delta = d(b,y) - d(a,x)$, we have $d(x,y) \leq \min\{d(a,b)+\Delta,\ d(a,b)-\Delta\} \leq d(a,b)$.

In particular, if x, y are diametrically opposite points, then $d(x,y) = d(a,b)$. Therefore, by Definition 3.1 the configuration (a,b) is extreme. □

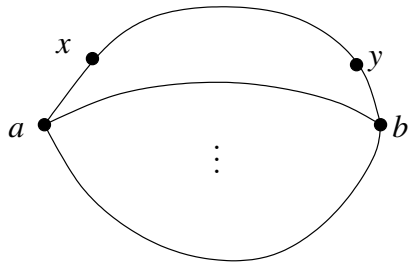

Figure 3.6: Points from small neighbourhoods of antipodal points a, b can be on the same path such as x, y.

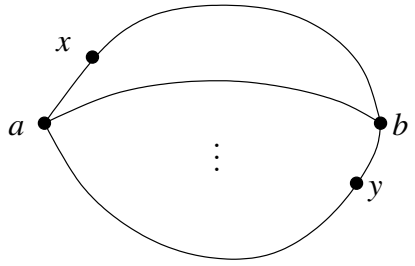

Figure 3.7: Points from small neighbourhoods of antipodal points a, b can be on different paths such as x, y.

Lemma 3.11. *If a configuration $(a,b) \in OC(G,2;r_1,r_2)$ is extreme, then a, b are vertices of degree one or a, b are antipodal points.*

Proof. By Definition 3.1 the configuration (a,b) is extreme if $d(a,b) \geq d(x,y)$ for all $x \in U_a$ and $y \in U_b$ where U_a, U_b are small neighbourhoods of a, b, respectively. For the

case when deg $a = \deg b = 1$, we acheive the desired conclusion that a, b are hanging vertices.

We will prove that (a,b) are antipodal by contradiction. Let us assume that at a there is an edge that does not belong to any path in $SP(a,b)$. It is possible to choose a point $x \in U_a$ on this edge close enough to x such that the shortest path between x, b includes one of the paths in $SP(a,b)$. So

$$d(x,b) = d(x,a) + d(a,b) > d(a,b)$$

which contradicts the assumption $d(x,y) \leq d(a,b)$ for all $(x,y) \in U_a \times U_b$.

Therefore, there is no edge at a or b which does not belong to the paths in the set $SP(a,b)$. Since in this case deg $a > 1$ and all edges at a belong to the paths in $SP(a,b)$, then $SP(a,b)$ has at least two elements. Therefore, a, b are antipodal points. □

Proposition 3.12. *A pair $(a,b) \in OC(G,2;r_1,r_2)$ is an extreme configuration if and only if a, b are hanging vertices or a, b are antipodal points.*

Proof. If $(a,b) \in OC(G,2;r_1,r_2)$ is an extreme configuration by Lemma 3.11, then a, b are vertices of degree one or a, b are antipodal points. The reverse follows from Lemma 3.9, Definition 3.6(2) and Lemma 3.10. □

3.3 Isolated extreme configurations

Lemma 3.13. *If a, b are antipodal points including exactly one hanging vertex, then $(a,b) \in OC(G,2;r_1,r_2)$ is an isolated extreme configuration.*

Proof. By Lemma 3.10 the pair (a,b) is extreme. Considering a as a hanging vertex, then G has the subgraph H shown in Fig. 3.8 containing at least two different paths α, β starting with different edges at b and finishing with the same hanging edge at a. For any $(x,y) \in U_a \times U_b$ where $x \neq a$, $y \neq b$, we have $d(x,y) < d(a,b)$. Therefore, the extreme configuration (a,b) is isolated by Definition 3.1. □

Lemma 3.14. *If antipodal points a, b are not hanging vertices and are not on the same topological circle, then (a,b) is an isolated extreme configuration.*

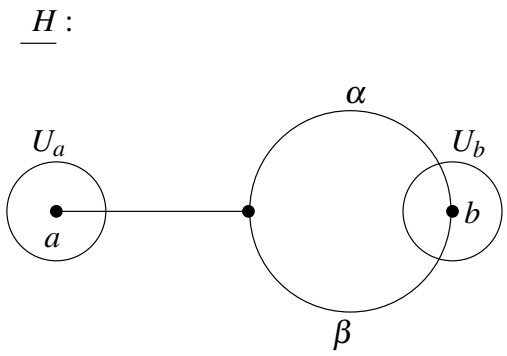

Figure 3.8: Subgraph H presents at least two different paths from a to b.

Proof. By Lemma 3.10 the pair (a,b) is extreme. For the antipodal points a, b, the graph G has the subgraph F shown in Fig. 3.9 containing at least two different paths α, β starting with different edges at a and finishing with two different edges at b. For any $(x,y) \in U_a \times U_b$, we have $d(a,b) > d(x,y)$, for $(x,y) \neq (a,b)$, so (x,y) is not extreme. Therefore, the extreme configuration (a,b) is isolated by Definition 3.1. □

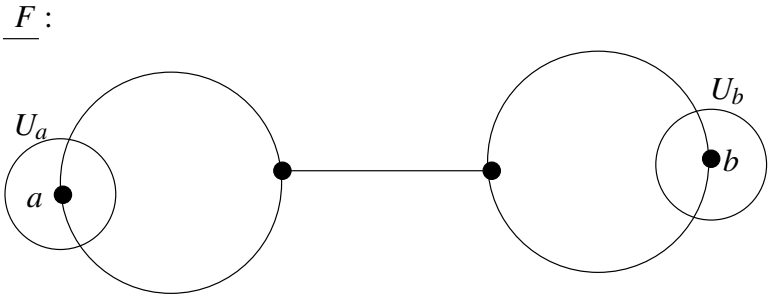

Figure 3.9: Subgraph F contains more than one path from a to b. See Lemma 3.10.

Example 3.15. In Fig. 3.10, the antipodal pair (a,b) is isolated. But in Fig. 3.11, the antipodal pair (c,d) is not isolated since c, d are on the same topological circle going through the vertices.

Example 3.16. In Fig. 3.12, consider the point a and its diametrically opposite point d. The configuration (a,d) is not extreme since it is possible to push a away from d within the edge e_1. Also, the configuration (b,c) is not extreme if the edge e between b, c does not belong to $SP(b,c)$. All pairs of diametrically opposite points on the circle excluding (a,d), (b,c) are extreme. All of these extreme configurations are non-isolated such as (x,y) since there are many extreme configurations in $U_x \times U_y$.

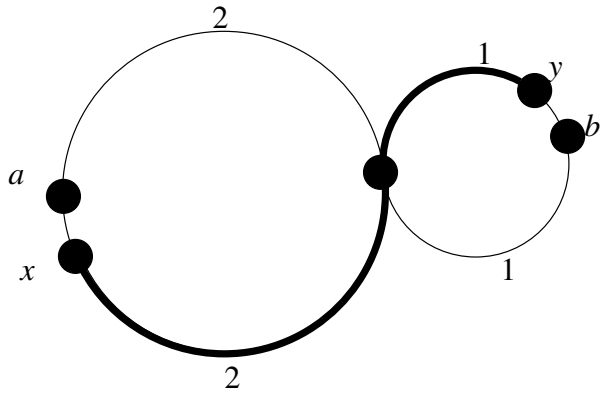

Figure 3.10: (a,b) is an isolated extreme configuration.

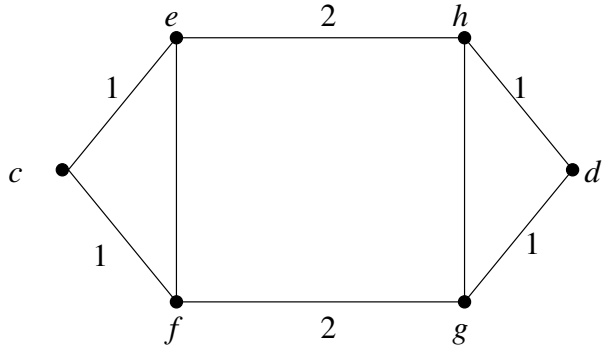

Figure 3.11: (c,d) is a non-isolated extreme configuration.

Proposition 3.17. *A configuration (a,b) is an isolated extreme configuration if and only if*
(1) *a, b are hanging vertices,*
(2) *a, b are antipodal points not on the same circle.*

Proof. If a, b are hanging vertices or if (a,b) are antipodal points not on the same circle, by Lemmas 3.9, 3.13 and 3.14, the configuration (a,b) is an isolated extreme configuration. The converse follows from Proposition 3.12, indeed, we exclude only antipodal points on the same circle. These are not isolated. □

3.4 An upper bound for path-connected components

Lemma 3.18. *If points a, b are diametrically opposite points of degree two on the same topological circle C of G, then (a,b) is a non-isolated extreme configuration.*

Proof. By Lemma 3.10 the configuration (a,b) is extreme. Consider any diametrically opposite points x, y that are sufficiently close to a, b, respectively, in the given circle

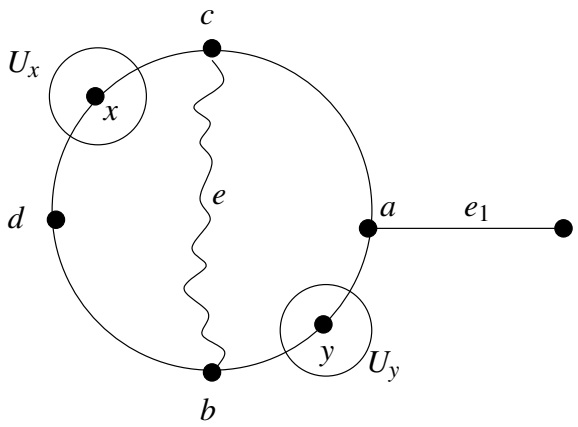

Figure 3.12: The edge e is longer than the semi circle. The configurations (a,d), (b,c) are not extreme. See Example 3.16.

C. Then x, y also have degree 2 and form an extreme configuration. Therefore, by Definition 3.1, the configuration (a,b) is not isolated. □

In the following example we will see that the reverse of the Lemma 3.18 is not always true.

Example 3.19. Consider the graph shown in Fig. 3.13. The extreme configuration (a,b) is non-isolated but a, b have degree 3, not 2.

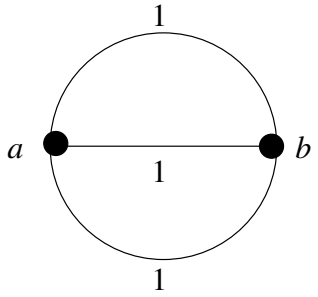

Figure 3.13: (a,b) is a non-isolated extreme configuration. See Example 3.19.

Lemma 3.20. *If (a,b) is a non-isolated extreme configuration then a, b are diametrically opposite points on the same topological circle.*

Proof. By Proposition 3.12, the points a, b are either hanging vertices or antipodal points. In Lemma 3.8, we discuss all different cases when a, b are antipodal. Proposition 3.17 excludes all cases except when the points a, b are diametrically opposite on the same topological circle of G. □

Example 3.21. Consider the graph G shown in Fig. 3.14. The configuration (x,y) of diametrically opposite points x, y is not extreme, since we can push the robots away along hanging edges. Similarly, the configurations (u,v), (w,z) are not extreme. But all other diametrically opposite points on the circle form non-isolated extreme configurations in $OC(G,2;r_1,r_2)$.

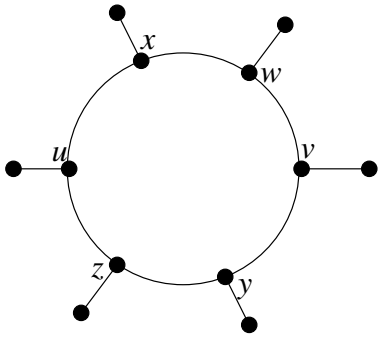

Figure 3.14: (x,y), (u,v), (w,z) are not extreme configurations. See Example 3.21.

Proposition 3.22. *All extreme configurations are either isolated extreme configurations or form punctured circles (with finitely many pairs of diametrically opposite points removed).*

Proof. By Lemma 3.18, diametrically opposite points of degree two on the same topological circle form a non-isolated extreme configuration. By Lemma 3.20, any non-isolated extreme configuration (a,b), consists of diametrically opposite points a, b on the same topological circle. □

Example 3.23. Consider the connected metric graph G shown in Fig. 3.15. Two robots with radii $r_1 = r_2 = 1$ are at the non-isolated extreme configuration (a,b). The configuration (c,d) is disjoint with the rest of the configuration space. So we can not continuously move the extreme configuration (a,b) to the isolated extreme configuration (c,d).

Definition 3.24. Denote by $EC(G,2;r_1,r_2)$ the number of all isolated extreme configurations plus the number of connected components of closures of punctured circles in the set of all extreme configurations.

Corollary 3.25. *The number of path-connected components of $OC(G,2;r_1,r_2)$ is not greater than $EC(G,2;r_1,r_2)$.*

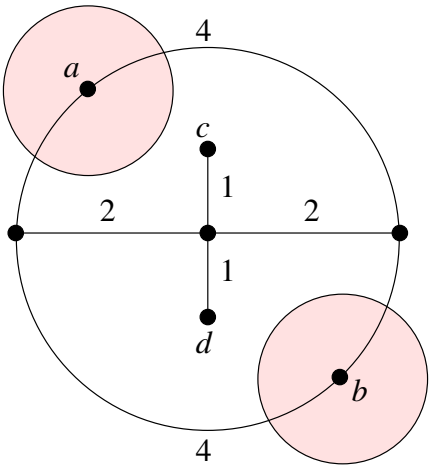

G

Figure 3.15: No continuous collision-free motion from (a,b) to (c,d). See Example 3.23.

Proof. By Proposition 3.16, each path-connected component of $OC(G,2;r_1,r_2)$ contains at least one extreme configuration. □

We label all vertices of a connected metric graph G by $v_1, v_2, \ldots v_n$. We represent G by its distance matrix $D(G)$ where each entry e_{ij} of $D(G)$ is the the length of the edge joining two adjacent vertices v_i, v_j. If there are multiple edges between vertices v_i, v_j in G, then we include the list of lengths of all edges for the entry e_{ij} of $D(G)$. The entry $e_{ij} = 0$ if the vertices v_i, v_j are not connected.

Example 3.26. The following distance matrix $D(G)$ illustrates the graph G in Fig. 3.16.

$$\begin{array}{c|cccc} & v_1 & v_2 & v_3 & v_4 \\ v_1 & 0 & 0 & 2 & 5 \\ v_2 & 0 & 0 & 2 & 0 \\ v_3 & 2 & 2 & 0 & 4 \\ v_4 & 5 & 0 & 4 & 2 \end{array} \tag{3.27}$$

The distance matrix $D(G)$ has only one row with one nonzero entry, so G has one hanging vertex. Moreover, the number of nonzero entries in each row shows the degree of the associated vertex. For any vertex, a nonzero entry at the diagonal of the matrix shows a loop at that vertex which will contribute two to the degree of the vertex.

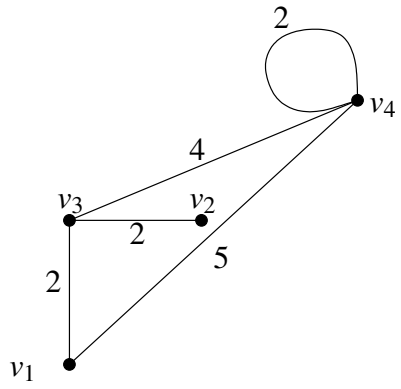

Figure 3.16: The graph G from Example 3.26.

We can find the number $EC(G,2;r_1,r_2)$ of any graph G algorithmically. The input of the algorithm is the distance matrix $D(G)$ and the output is $EC(G,2;r_1,r_2)$. This result reduces the path-connectivity problem for the configuration space $OC(G,2;r_1,r_2)$ to a finite set of extreme configurations $EC(G,2;r_1,r_2)$ (all isolated extreme configurations plus one configuration from each punctured circle). But we could not find a way to decide whether two extreme configurations are in the same path-connected component of $OC(G,2;r_1,r_2)$. To find the number of path-connected components of the configuration space $OC(G,2;r_1,r_2)$, we shall follow a different approach in Chapter 4.

Chapter 4

Configuration skeletons of graphs

4.1 The configuration skeleton of a graph

In this chapter we consider two robots with radii $r_1,\ r_2 > 0$ on a connected metric graph G. We define the configuration skeleton $CS(G,2;r_1,r_2)$ as an special subgraph in $OC(G,2;r_1,r_2)$. We shall show later in Theorem 4.13 that $CS(G,2;r_1,r_2)$ has the same number of path-connected components as $OC(G,2;r_1,r_2)$.

Definition 4.1. Let G be a connected metric graph. We assume that any vertex on a topological circle $C \subset G$ has a diametrically opposite vertex, otherwise, we add the diametrically opposite vertex of degree two to the circle C. The *configuration skeleton* of $OC(G,2;r_1,r_2)$, denoted as $CS(G,2;r_1,r_2)$, is the following combinatorial graph whose vertices are all pairs (u,v), where u, v are vertices of G and the distance $d(u,v) \geq r_1 + r_2$.
(1) We connect vertices (v,u), (w,u) by an edge in $CS(G,2;r_1,r_2)$ if v, w are connected by an edge in G. (Similarly, we connect the vertices (u,v), (u,w).)
(2) We connect vertices (u,v), (w,z) by an edge in $CS(G,2;r_1,r_2)$ if

- u, w, are adjacent vertices on a topological circle $C \subset G$, and
- v, z, are adjacent vertices on the same topological circle $C \subset G$, and
- $d(u,z) < r_1 + r_2$, $d(v,w) < r_1 + r_2$, see Fig. 4.2.

Example 4.2. Let the metric graph G be a circle with two diametrically opposite vertices u, v as shown in Fig. 4.1. If $0 < r_1 + r_2 \leq 1$, the configuration skeleton $CS(G,2;r_1,r_2)$ has

two vertices (u,v), (v,u) that are connected by two edges as defined in Definition 4.1(2). This is a particular case when $w = v$, $z = u$. Robot 1 moves clockwise from u to v and simultaneously, robot 2 moves clockwise from v to u. Similarly, robot 1 moves counterclockwisely from u to v and simultaneously, robot 2 moves counterclockwisely from v to u. If $1 < r_1 + r_2$, the configuration space $OC(G,2;r_1,r_2)$ is empty, so is $CS(G,2;r_1,r_2)$.

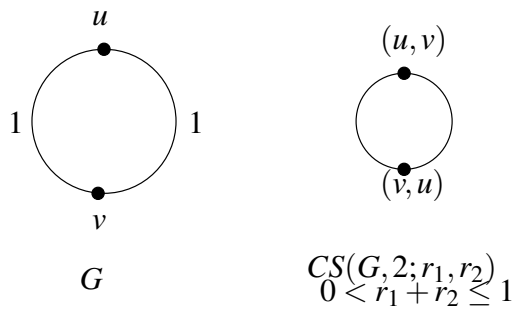

Figure 4.1: The configuration skeleton is a circle. See Example 4.2.

Example 4.3. Consider the circle G with four vertices as shown in Fig. 4.2. If $2 < r_1 + r_2 \leq 3$, the configuration skeleton $CS(G,2;r_1,r_2)$ has four vertices. By Definition 4.1(2), the vertices (u,w), (v,z) are connected with an edge. Similarly, the vertices (u,w), (z,v) are connected with an edge. symmetrically, the vertices (w,u), (v,z) are connected with an edge. Also the vertices (w,u), (z,v) are connected with an edge. Therefore the configuration skeleton $CS(G,2;r_1,r_2)$ is a circle as shown in Fig. 4.2.

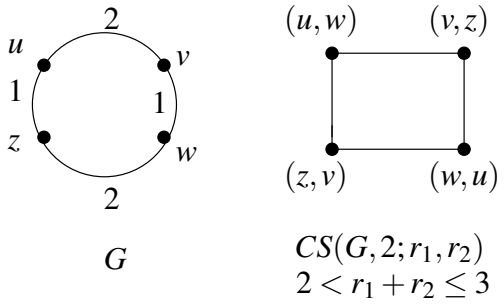

Figure 4.2: If $2 < r_1 + r_2 \leq 3$, the configuration skeleton is a circle. See Example 4.3.

If $0 < r_1 + r_2 \leq 1$, the configuration skeleton has twelve vertices, as shown in Fig. 4.3. In this case, since the distance between any two vertices of G is greater or equal to $r_1 + r_2$,

the vertices in $CS(G,2;r_1,r_2)$ are connected by an edge if Definition 4.1(1) is satisfied. For example, the vertices (u,v), $(u,,w)$ are connected with an edge since v, w are adjacent in G. If $1 < r_1 + r_2 \leq 2$, the configuration skeleton does not have the vertices (u,z), (w,v), (v,w), (z,u). So either the vertices (u,w), (u,v) are connected by an edge by Definition 4.1(1), or the vertices (u,w), (v,z) are connected by an edge by Definition 4.1(2). The resulting configuration skeleton is shown in Fig. 4.3.

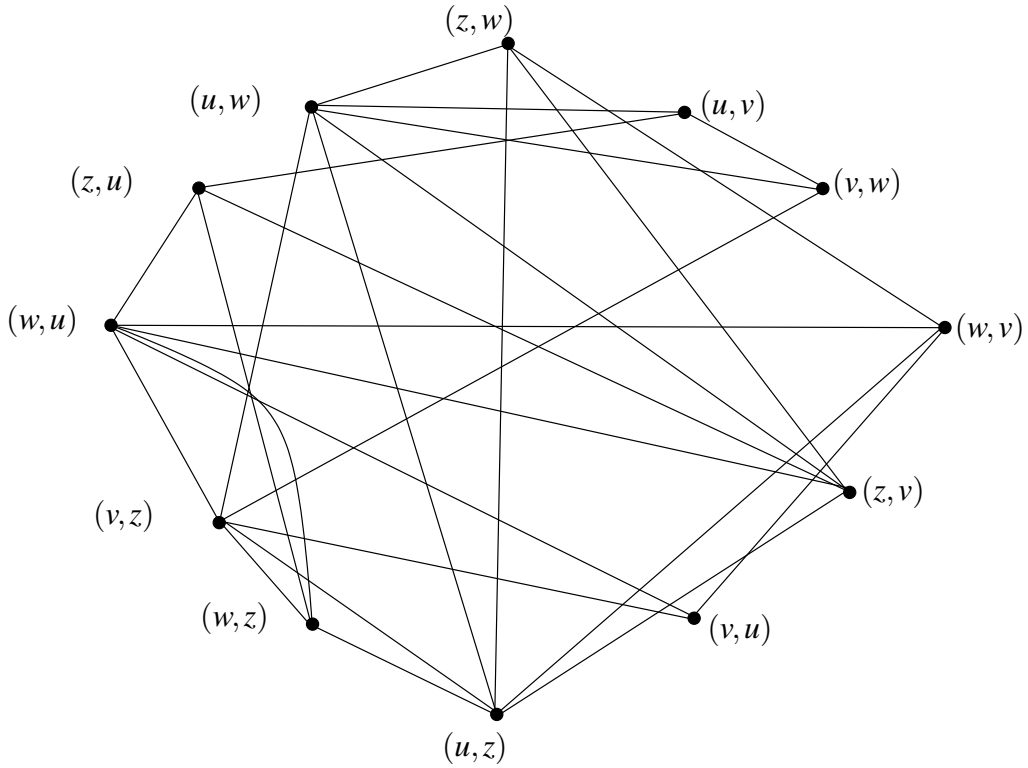

$CS(G,2;r_1,r_2)$
$0 < r_1 + r_2 \leq 1$

Figure 4.3: Configuration skeleton for $0 < r_1 + r_2 \leq 1$. See Example 4.3.

Example 4.4. Consider the metric graph G with three edges and three vertices as shown in Fig. 4.5. The distance $d(v_i,v_j) \geq 1$ for $i = 1,2,3$ and $j = 1,2,3$. If $0 < r_1 + r_2 \leq 1$, the configuration skeleton $CS(G,2;r_1,r_2)$ has six vertices. Since the vertices v_1, v_2 are on the same topological circle, by Definition 4.1(2), the vertices (v_1,v_2), (v_2,v_1) are connected by an edge in $CS(G,2;r_1,r_2)$. Also if a robot is fixed at v_1, we can move the second robot from v_2 to v_3. So the vertices (v_1,v_2), (v_1,v_3) are connected by an edge

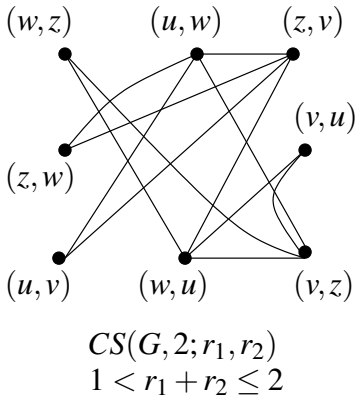

Figure 4.4: Configuration skeleton for $1 < r_1 + r_2 \leq 2$. See Example 4.3.

in $CS(G,2;r_1,r_2)$. Finally, we fix second robot at v_3 and move the first robot from v_1 to v_2, by Definition 4.1(1). So the vertices (v_1,v_3), (v_2,v_3) are connected by an edge in $CS(G,2;r_1,r_2)$. Symmetrically, the remaining two vertices are connected by an edge to this graph as shown in Fig. 4.5 (middle). If $1 < r_1 + r_2 \leq 2$, a robot can not stand at v_2, so $CS(G,2;r_1,r_2)$ has two isolated vertices as shown in Fig. 4.5 (right). The vertex (v_1,v_3), (v_3,v_1) are not connected since v_1, v_3 are not adjacent and are not on a topological circle.

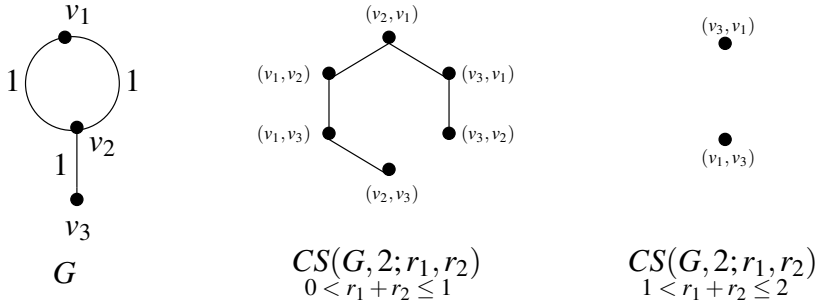

Figure 4.5: The configuration skeletons of graph G. See Example 4.4.

Example 4.5. Consider the wedge G of two circles as shown in Fig. 4.6. If $0 < r_1 + r_2 \leq 1$, similar to the Example 4.4, the configuration skeleton $CS(G,2;r_1,r_2)$ consists of six vertices. By Definition 4.1(2), the vertices (v_2,v_3), (v_3,v_2) are connected by an edge, since v_2, v_3 are on the same circle as shown in Fig. 4.6 (middle). If $1 < r_1 + r_2 \leq 2$, the configuration skeleton $CS(G,2;r_1,r_2)$ has two isolated vertices as shown in Fig. 4.6 (right).

Example 4.6. Consider the metric graph G with 4 vertices and three edges with length 1 as shown in Fig. 4.7. If $0 < r_1 + r_2 \leq 1$, the configuration skeleton $CS(G,2;r_1,r_2)$ consists

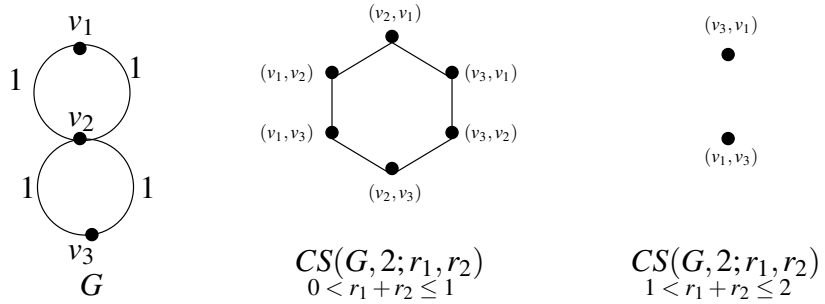

Figure 4.6: The configuration skeletons of graph G. See Example 4.5.

of 12 vertices as shown in Fig. 4.7 (middle). By Definition 4.1(1), a robot is fixed at vertex v_1, and the other robot is moved along one edge from v_2 to v_3. Similarly, we continue by fixing one robot at a vertex and move the second robot along an edge. For $1 < r_1 + r_2 \leq 2$, the configuration skeleton $CS(G,2;r_1,r_2)$ has six isolated vertices since there is not any pair of adjacent vertices in G, as shown in Fig. 4.7 (right).

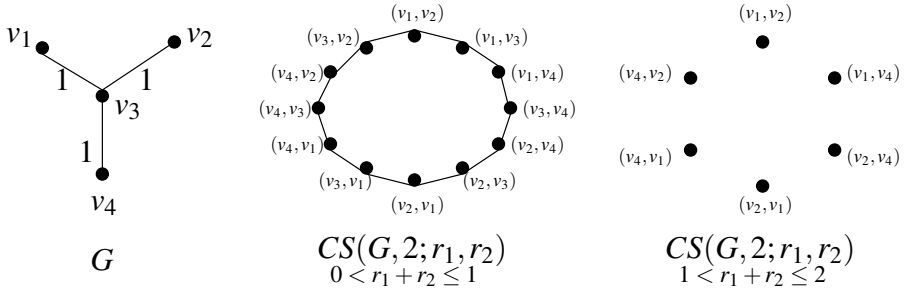

Figure 4.7: The configuration skeletons of graph G. See Example 4.6.

Example 4.7. Consider the metric graph G with four vertices and three edges with different lengths as shown in Fig. 4.8 (left). If $0 < r_1 + r_2 \leq 1$, the configuration skeleton $CS(G,2;r_1,r_2)$ has 12 vertices. Similarly to Example 4.6, if $1 < r_1 + r_2 \leq 2$, by fixing a robot at vertex v_1, the other robot can not stand on v_3. So $CS(G,2;r_1,r_2)$ has 10 vertices and 8 edges as shown in Fig. 4.8 (top-right). If $2 < r_1 + r_2 \leq 3$, fixing a robot at v_3, the other robot can only stand on v_4. So $CS(G,2;r_1,r_2)$ has 8 vertices and four edges. By Definition 4.1, the vertices (v_1,v_4), (v_3,v_4) are connected by an edge in $CS(G,2;r_1,r_2)$, Similarly, the vertices (v_3,v_4), (v_2,v_4) are connected by an edge as shown in Fig.4.8 (bottom-left). For $3 < r_1 + r_2 \leq 4$, the configuration skeleton $CS(G,2;r_1,r_2)$ has four isolated vertices since, robots can not stand on v_3. Finally, for $4 < r_1 + r_2 \leq 5$, the configuration skeleton $CS(G,2;r_1,r_2)$ has two isolated vertices (v_2,v_4), (v_4,v_2) as shown in

Fig. 4.8 (bottom-right).

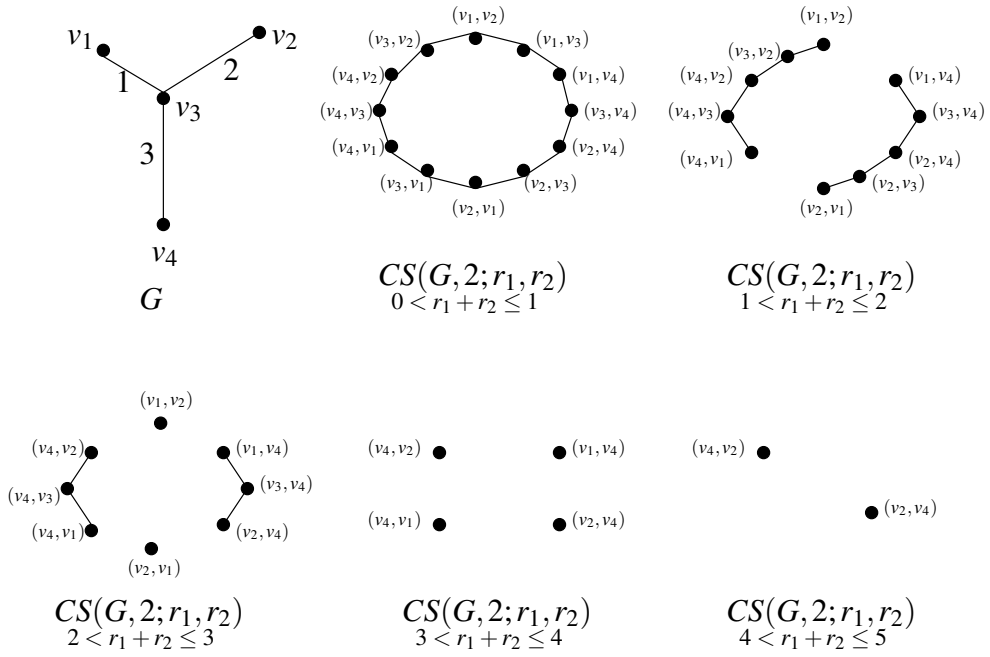

Figure 4.8: The configuration skeletons of graph G. See Example 4.7.

4.2 Elementary motions

Lemma 4.8. *There is a path from any configuration $(x,y) \in OC(G,2;r_1,r_2)$ to a vertex $(u,v) \in CS(G,2;r_1,r_2)$.*

Proof. The nontrivial case is when (robot 1 at) x or (robot 2 is at) y is not at a vertex of G. Consider x is at a vertex, then push y away from x until y reaches a vertex. Assuming x, y are diametrically opposite on the same topological circle, then keeping x fixed and pushing y away will only decrease $d(x,y)$. But by our assumption, we have added a diametrically opposite vertex to each vertex on any topological circle of G. □

Definition 4.9. An *elementary* motion in $OC(G,2;r_1,r_2)$ is defined as follows.
(1) Let u, v, $w \in G$ be vertices. For instance, see Fig. 4.9(1). If

- v, w are connected with an edge in G, and
- $d(v,w) \geq r_1 + r_2$,

then the motion from (u,v) to (u,w) is called *elementary*. This means the first robot is fixed at vertex u and the second robot moves from v to the adjacent vertex w. (Similarly, we define an *elementary motion* from (v,u) to (w,u)).

(2) Let the vertices u, v, w, z be on a topological circle $C \in G$, see Fig. 4.9(2). If

- $d(u,v) \geq r_1 + r_2$, $d(w,z) \geq r_1 + r_2$, and
- u is adjacent to w and v is adjacent to z,

then we can move the first robot from u to w and simultaneously, the second robot from v to z in the same direction on the topological circle $C \in G$ without collisions. This motion is also called an *elementary motion*.

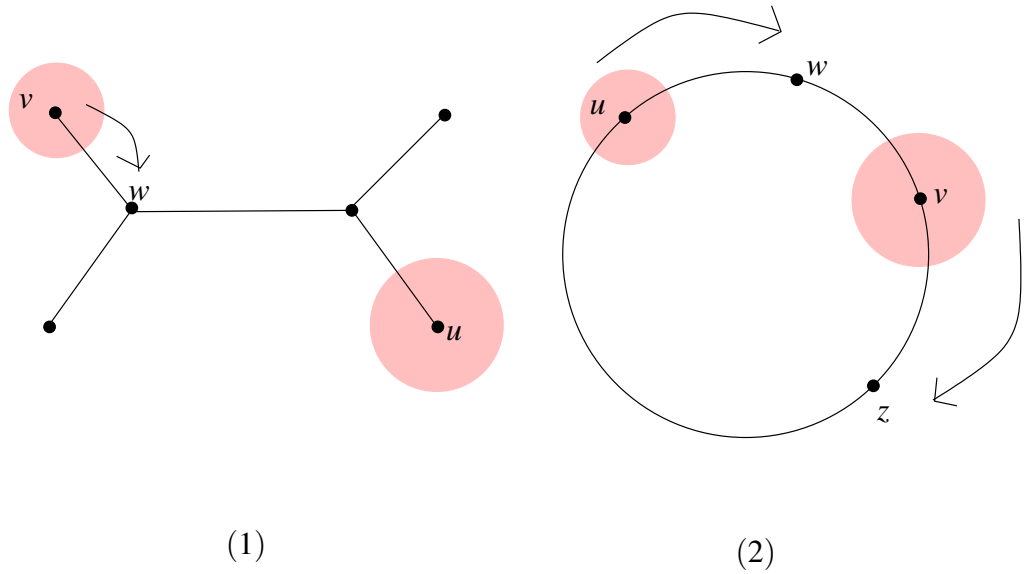

Figure 4.9: Two types of elementary motion. See Definition 4.9.

Lemma 4.10. *The configuration skeleton $CS(G,2;r_1,r_2)$ can be considered as an embedded topological graph in $OC(G,2;r_1,r_2)$.*

Proof. By Definition 4.1, all vertices of the configuration skeleton $CS(G,2;r_1,r_2)$ are configurations in $OC(G,2;r_1,r_2)$. By Definitions 4.1 and 4.9, every edge in $CS(G,2;r_1,r_2)$ between two vertices is an elementary motion between the same configurations in $OC(G,2;r_1,r_2)$. Any two edges in $CS(G,2;r_1,r_2)$ may meet only at vertices as desired. □

Lemma 4.11. *Let u, v, w, z be vertices of G. Assume that there is a collision-free motion from (u,v) to (w,z), where u is adjacent to w and v is adjacent to z. If $d(u,z) \geq r_1 + r_2$*

or $d(w,v) \geq r_1 + r_2$, then the motion can be replaced by two elementary motions without collisions.

Proof. Assuming that $d(w,v) \geq r_1 + r_2$, we fix robot 2 at v and move robot 1 from u to w, see Fig. 4.9(2). Then we fix robot 1 at w and move robot 2 from v to z. If $d(u,z) \geq r_1 + r_2$, we fix robot 1 at u and move robot 2 from v to z. Then we fix robot 2 at z and move robot 1 from u to w. So we have the motion from (u,v) to (w,z) either via (w,v) or via (u,z). □

The assumptions of Lemma 4.12 below will hold in case (2) of Theorem 4.13. We recall that any vertex on a topological circle $C \subset G$ has a diametrically opposite vertex, otherwise, we add a diametrically opposite vertex of degree 2 to the circle C.

Lemma 4.12. *Let v, w be vertices of G, and $z \in G$ not be a vertex. Assume that $d(w,z) \geq r_1 + r_2 > d(w,v)$. Let the vertex $q \in G$ be connected to v by the edge that contains z. Then we have $d(w,q) \geq r_1 + r_2$ (see Fig. 4.10).*

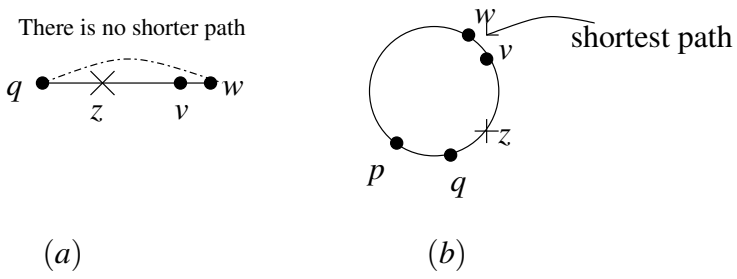

Figure 4.10: (a) illustrates case (1), and (b) illustrates case (2) in Lemma 4.12.

Proof. Case (1) : assume v, w, q are not on any topological circle as shown in Fig. $4.10(a)$. We denote z by a cross. Connect the vertices v, w by a shortest path, see Fig. 4.10(a). Then the shortest path from w to q is via the vertex v and the point z. Then we have $d(w,q) = d(w,z) + d(z,q) > r_1 + r_2$ by the given inequality $d(w,z) \geq r_1 + r_2$. Otherwise, we get a circle containing v, w, q.

Case (2) : assume v, w, q are on a topological circle $C \subset G$. Let p be the diametrically opposite vertex to w on C as shown in Fig. $4.10(b)$. Hence the distance between w, p is the largest distance between any points on C, so $d(w,p) \geq d(w,q)$. Since, the vertex p can not be inside the edge with the endpoints q, v. It is given that $d(w,z) \geq r_1 + r_2 > d(w,v)$, then either $q = p$ or q is the shortest arc of C between p and z. Then $d(w,q) > d(w,z) \geq r_1 + r_2$.

□

Let us remind that we consider only collision-free motions. This means two robots can only intersect at one point when the distance between two robots is $r_1 + r_2$. It is important to remember that the robots are metric balls. See Definition 2.23 for more details.

Theorem 4.13. *We assume that G is a connected metric graph and any vertex on a topological circle $C \subset G$ has a diametrically opposite vertex, otherwise, we add the diametrically opposite vertex of degree two to the circle C. Then any collision-free motion $(x(t), y(t))$, $0 \leq t \leq 1$, where $x(0)$, $y(0)$, $x(1)$, $y(1)$ are vertices of G, can be replaced by a finite sequence of elementary motions.*

Proof. We prove the theorem by induction on the number k of vertices in G that at least one of the robots visits during the motion $(x(t), y(t))$, $0 \leq t \leq 1$. Vertices are counted with multiplicities, i.e. when in a motion a robot visits the same vertex m times over $0 < t < 1$, then we count this vertex m times. But the initial and the final vertices $x(0)$, $y(0)$, $x(1)$, $y(1)$ are not counted.

Induction base: $(k = 0)$ If the robots do not visit any vertices over $0 < t < 1$, then robot 1 moves along one edge and robot 2 moves simultaneously along another edge. There are the following two cases.

Case (1) : let $d(x(0), y(1)) \geq r_1 + r_2$ or $d(x(1), y(0)) \geq r_1 + r_2$. Then the motion from $(x(0), y(0))$ to $(x(1), y(1))$ can be replaced by two elementary motions by Lemma 4.11, where $u = x(0)$, $v = y(0)$, $w = x(1)$, $z = y(1)$.

Case (2) : let $d(x(0), y(1)) < r_1 + r_2$ and $d(x(1), y(0)) < r_1 + r_2$. Then by Definition 4.9(2), the motion from $(x(0), y(0))$ to $(x(1), y(1))$ is elementary. So the induction base $k = 0$ is complete.

Inductive assumption: let the theorem hold for all motions when both robots visit at most k vertices of G, counted with multiplicities.

Inductive step: We prove the theorem for a motion when both robots visit exactly $k + 1$ vertices of G. We consider the time interval from 0 to the first moment $t \in (0, 1)$, when one of the robots reaches a vertex, say robot 1. So robot 1 moves from the vertex $x(0)$ to an adjacent vertex $x(t)$, and robot 2 moves from the vertex $y(0)$ to a point $y(t)$, not a vertex. There are no vertices between $y(0)$, $y(t)$. We have the following cases.

Case(1) : let $d(x(t), y(0)) \geq r_1 + r_2$.

- We fix robot 2 at $y(0)$ and move robot 1 from $x(0)$ to $x(t)$. This elementary motion from $(x(0),y(0))$ to $(x(t),y(0))$ is collision-free since $y(0)$ is far away from both points $x(0)$ and $x(t)$.

- Then we fix robot 1 at $x(t)$ and move robot 2 from $y(0)$ to $y(t.)$ This motion from $(x(t),y(0))$ to $(x(t),y(t))$ is collision-free since $x(t)$ is far away from both points $y(0)$ and $y(t)$.

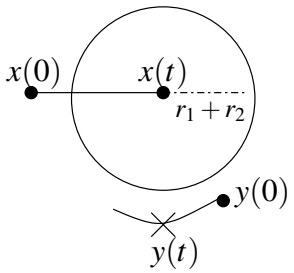

Figure 4.11: The figure illustrates case (1), when $y(0)$, $x(t)$ are far away.

After that the robots move from $(x(t),y(t))$ to $(x(1),y(1))$ as in the original motion. During the motion from $(x(t),y(0))$ to $(x(1),y(1))$, the robots visit only k vertices because the vertex $x(t)$ is not counted anymore as the initial position of robot 1, see in Diagram 1. So the inductive step is finished in case (1), as shown in Diagram(1).

$$\overbrace{(x(0),y(0)) \xrightarrow[\text{elementary}]{} (x(t),\underbrace{y(0)) \xrightarrow[\text{non-elementary}]{} (x(t),y(t)\overbrace{) \to \cdots \to (}^{\text{unchanged}}x(1),y(1))}_{k \text{ vertices to visit, shorter collision-free motion}}}^{\text{original collision-free motion}}$$

Diagram (1)

We apply Lemma 4.12 for $v = y(0)$, $w = x(t)$, $z = y(t)$. The assumptions of Lemma 4.12 hold since

- $x(0)$, $y(0)$, $x(t)$ are vertices of G, and

- the point $y(t) \in G$ is not a vertex, and

- the vertex $x(0)$ is adjacent to $x(t)$, and

- there is no vertex between $y(0)$ and $y(t)$, and
- we have $d(x(t),y(0)) < r_1 + r_2$.

Let q be the adjacent vertex to $y(0)$ by the edge that contains $y(t)$. The condition

$$d(w,z) = d(x(t),y(t)) \geq r_1 + r_2$$

in Lemma 4.12 holds, because the robots at time t do not collide. Lemma 4.12 implies that $d(q,x(t)) \geq r_1 + r_2$, for $w = x(t)$, $v = y(0)$, $z = y(t)$.

Case(2) : let $d(x(t),y(0)) < r_1 + r_2$ and $d(q,x(0)) \geq r_1 + r_2$.

- We fix robot 1 at $x(0)$ and push robot 2 from $y(0)$ to q. So the elementary motion $(x(0),y(0))$ to $(x(0),q)$ is collision-free since $x(0)$ is far away from both points $y(0)$, q.
- Then we fix robot 2 at q and push robot 1 from $x(0)$ to $x(t)$. The elementary motion from $(x(0),q)$ to $(x(t),q)$ is collision-free since q is far away from $x(0)$, $x(t)$.
- We now fix robot 1 at $x(t)$ and push robot 2 back from q to $y(t)$. This motion from $(x(t),q)$ to $(x(t),y(t))$ is collision-free since $x(t)$ is far away from both q, $y(t)$.

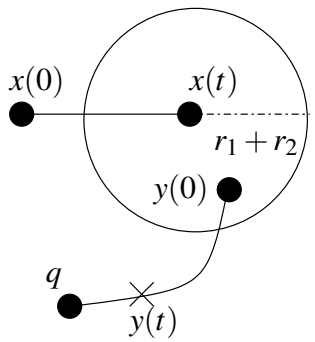

Figure 4.12: Case (2), when $y(0)$, $x(t)$ are close, but q, $x(0)$ are far away.

After that we have the original motion from $(x(t),y(t))$ to $(x(1),y(1))$. During the motion from $(x(t),q)$ to $(x(1),y(1))$, the robots visit only k vertices because the vertex $x(t)$ is not counted anymore as the initial position of robot 1, see in Diagram 2. So the inductive step is finished in case (2).

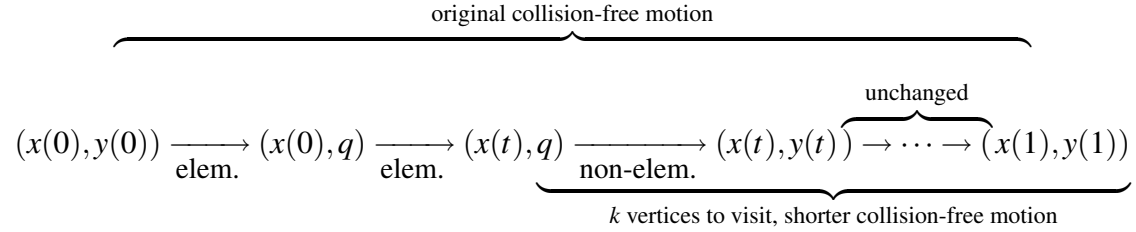

Diagram (2)

Case (3) : Let $d(x(t),y(0)) < r_1 + r_2$ and $d(q,x(0)) < r_1 + r_2$. Then $x(0)$, $y(0)$, $x(t)$, $y(t)$ are on a topological circle $C \subset G$, similar to the example 4.3.

- Then we move robot 1 from $x(0)$ to $x(t)$, simultaneously, we move robot 2 from $y(0)$ to q. By Definition 4.9(2), the elementary motion from $(x(0),y(0))$ to $(x(t),q)$ is collision-free since $x(t)$, q are far away.

- Then we fix robot 1 at $x(t)$ and move robot 2 back from q to $y(t)$. The motion from $(x(t),q)$ to $x(t),y(t)$ is collision-free since $x(t)$, $y(t)$ are far away.

After that we have the original motion from $(x(t),y(t))$ to $(x(1),y(1))$. During the motion from $(x(t),q)$ to $(x(1),y(1))$, the robots visit only k vertices because the vertex $x(t)$ is not counted anymore as the initial position of robot 1, see in Diagram(3). So the inductive step is finished in case (3).

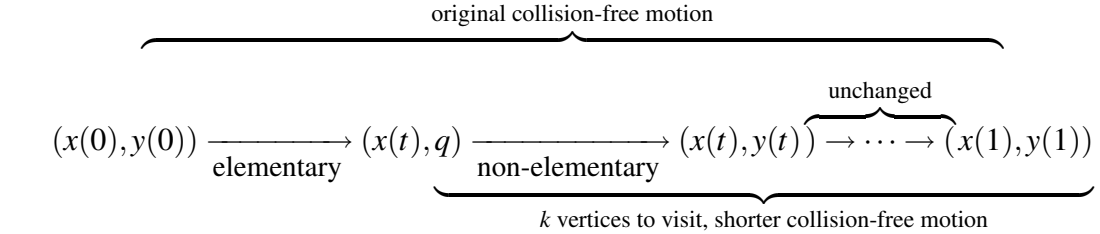

Diagram (3)

□

We illustrate Theorem 4.13 in a simple case when two robots u, v are far away from each other, Namely, $d(u,v) \geq r_1 + r_2$. In this case, u, v aim to move to w, z, respectively, where $d(w,z) \geq r_1 + r_2$.

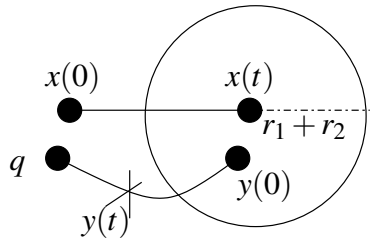

Figure 4.13: Case (3), when $y(0)$, $x(t)$ are close, and q, $x(0)$ are close too.

Example 4.14. For instance, consider two robots with radii $\frac{1}{2}$, $\frac{1}{3}$ on the connected metric graph G shown in Fig. 4.14. We can fix robot 1 at u and move robot 2 from v to z without any collisions. Then we fix robot 2 at z and move robot 1 from u to w. This collision-free motion from (u,v) to (w,z) consists of six elementary motions.

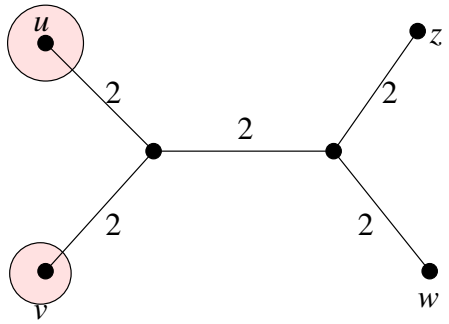

G

Figure 4.14:

In the following lemma, we will see generalisation of the argument above.

Lemma 4.15. *If vertices $v, w \in G$ are in the same component of the complement $G - B(u, r_1 + r_2)$ of the open ball $B(u, r_1 + r_2)$ with the centre u and radius $r_1 + r_2$, then (u,v), (u,w) are in the same component of $CS(G, 2; r_1, r_2)$.*

Proof. Take a path from v to w in $G - B(u, r_1 + r_2)$. Then adding the fixed robot at u, we get a sequence of elementary motions from (u,v) to (u,w) by Definition 4.9. □

4.3 Conclusion about path-connectivity

The following corollary is the main result of this chapter.

Corollary 4.16. *We assume that G is a connected metric graph and any vertex on a topological circle $C \subset G$ has a diametrically opposite vertex, otherwise, we add the diametrically opposite vertex of degree two to the circle C. Then there is a* $1-1$ *correspondence between all path-connected components of* $OC(G,2;r_1,r_2)$ *and all path-connected components of* $CS(G,2;r_1,r_2)$.

Proof. By Definition 4.1, each vertex $(u,v) \in CS(G,2;r_1,r_2)$, is a configuration in $OC(G,2;r_1,r_2)$. By Theorem 4.13, if two such configurations are in the same path-connected component of $OC(G,2;r_1,r_2)$, they are connected by finitely many elementary motions, hence they are connected by finitely many edges in $CS(G,2;r_1,r_2)$. Indeed, by Lemma 4.10, if there is an edge between two vertices in $CS(G,2;r_1,r_2)$, the corresponding configurations are connected in $OC(G,2;r_1,r_2)$ by an elementary motion. □

In the Corollary 4.16, we have seen that $CS(G,2;r_1,r_2)$, $OC(G,2;r_1,r_2)$ have the same number of path-connected components. In the following, we investigate if the fundamental group of $CS(G,2;r_1,r_2)$ is isomorphic to the fundamental group of $OC(G,2;r_1,r_2)$. If the graph $CS(G,2;r_1,r_2)$ is connected, then the fundamental group of $CS(G,2;r_1,r_2)$ is free. We have seen in Example 2.37 that the fundamental group of $OC(K_5,2;r_1,r_2)$ for small radii r_1, r_2 is not free. So we conclude that $CS(G,2;r_1,r_2)$ has the same π_0-group (the number of path-connected components) as $OC(G,2;r_1,r_2)$, but may not have the same fundamental π_1-group.

The main aim of this thesis was to compute the number of path-connected components of the configuration space $OC(G,2;r_1,r_2)$ of two metric balls on a metric graph G. In sections 2.1, 2.2, we started by reviewing the results of the simpler model of the configuration space of two zero-sized robots on a graph. In chapter 3, we represented the finite set $CEC(G)$ of extreme configurations that are connected to all other configurations by some paths in $OC(G,2;r_1,r_2)$. In other words, in each path-connected component of $OC(G,2;r_1,r_2)$, there is at least one element of $CEC(G)$. Though, we could not find a method to connect extreme configurations of the same path-connected component.

In order to compute the number of path-connected components of $OC(G,2;r_1,r_2)$, we introduced a new technique. In this technique, we consider all configurations (u,v), where both u, v are vertices in G. Namely, we do not consider the configurations when at least

one robot is on the edge of G. Then we define a collision-free elementary motion that any collision-free motion of two robots in $OC(G,2;r_1,r_2)$ could be replaced by a sequence of such elementary motions.

References

[1] A. Abrams (2000), *Configuration spaces and braid groups of graphs*. PhD thesis, University of California at Berkeley. Available at: `http://www.mathcs.emory.edu/~abrams/research/Papers/index.html`.

[2] A. Abrams, D. Gay and V. Hower (2010), *Discretized configurations and partial partitions*. Available at: `arXiv:1009.2935v1`.

[3] K. Barnett and M. Farber (2009), *Topology of configuration spaces of two particles on a graph, I*. Algebraic and Geometric Topology, Volume 9, Issue 1, Page 593-624. Available at: `arXiv:0903.2180v1`.

[4] *Topology and Its Applications* Available at: http://people.rit.edu/wfbsma/topology_and_its_applications/links.html Including: `http://www.cs.colorado.edu/~lizb/topology.html`

[5] F. Connolly and M. Doig (2004), *Braid groups and right angled Artin groups*. `arXiv:math/0411368v1`.

[6] K. Deeley (2011), *Configuration spaces of thick particles on graphs*. PhD thesis, Durham University. Available at: `http://etheses.dur.ac.uk/862/`.

[7] M. Farber (2005), *Collision free motion planning on graphs*. in: "Algorithmic Foundations of robotics IV", M. Erdmann, D. Hsu, M. Overmars, A. Frank van der Stappen editors, Springer, Page 123-138. Available at: `arXiv:math/0406361v1`.

[8] M. Farber (2008), *Invitation to topological robotics*. European Mathematical Society.

[9] M. Farber and E. Hanbury (2010), *Topology of configuration space of two particles on a graph ,II*. Algebraic and Geometric Topology, Volume 10, Issue 4, Page 2203-2227. Available at: `arXiv:1005.2300v1`.

[10] D. Farley and L.Sabalka (2008), *On the cohomology rings of tree braid groups*. Journal of Pure and Applied Algebra Volume 212, Page 53-71. Available at: `arXiv:math/0602444v2`.

[11] D. Farley and L. Sabalka (2001), *Discrete Morse theory and graph braid groups*. Algebraic & Geometric Topology 5, 2005, Page 1075-1109.

[12] R. Ghrist and D. Koditschek (1998), *Safe cooperative robot motions via dynamics on graphs*. Eighth Intl. Symp. on Robotic Research, Y. Nakayama, ed., Springer-verlag, Page 81-92. Available at: `http://www.math.uiuc.edu/~ghrist/preprints/AGV.pdf`.

[13] R. Ghrist (2001), *Configuration spaces and braid groups on graphs in robotics, in Braids, Links, and Mapping Class Groups: the Proceedings of Joan Birman's 70th Birthday*. AMS/IP Studies in Mathematics, Volume 24, Page 29-40. Available at: `arXiv:math/9905023v1`.

[14] R. Ghrist and D. Koditschek (2002), *Safe, cooperative robot dynamics on graphs*. SIAM J. Control and Optimization, $40(5)$, $1556-1557$. Available at: `arXiv:cs/0002014v1`.

[15] R. Ghrist (2007), *Configuration spaces, braid and robotics*. Survey for summer school on braids and applications at the National University of Singapore. Avaiable at: `http://www.math.uiuc.edu/~ghrist/preprints/singaporetutorial.pdf`.

[16] A. Hatcher (2002), *Algebraic topology*. Cambridge University Press. Available at: `http://www.math.cornell.edu/~hatcher/`.

[17] N. G. Hockstein, C. G. Gourin, R. A. Faust, D. J. Terris (2007), *A history of robots: from science fiction to surgical robotics*, Review article, available at: `http://download.springer.com/static/pdf/324/`

art%253A10.1007%252Fs11701-007-0021-2.pdf?auth66=1360337377_26f5069b27ce5eed26b15d3a1522ba67\&ext=.pdf.

[18] C. Kassel and V. Turaev (2008), *Braid Groups*. Graduate Texts in Mathematics, 247. Springer, New York, 2008. xii+340 pp. ISBN: 978-0-387-33841-5 (Reviewer: Stephen P. Humphries) 20F36 (20C08 20F10 20F60 20M05 55R80 57M25 57M50)

[19] Ki Hyoung Ko and Hyo Won Park (2011), *Characteritics of graph braid groups*. Available at: arXiv:1101.2648v1.

[20] V. Kurlin (2009), *Computing braid groups of graphs with applications to robot motion planning*. Homology, Homotopy and Applications, Volume 14, 2012. No. 1, Page 159 – 180. Available at: arXiv:0908.1067v1.

[21] S. M. LaValle (2006), *Planning Algorithms*. Cambridge University press. Available at: http://planning.cs.uiuc.edu.

[22] J. R. Munkres (2003), *Topology a first course*, 1975 by Prentice-Hall.

[23] A. Neels and S. Privitera (2005), *Braid groups of the sun graph*. Available at: arXiv:math/0508380v1.

[24] P. Prue and T. Scrimshaw (2009), *Abram's stable equivalence for graph braid groups*. Available at: arXiv:0909.5511v1.

[25] K. H. Rosen (2000), *Handbook of Discrete and Combinatorial Mathematics*. (2000) by CRC Press.

[26] H. Sadofsky, *Fundamental group of wedge of circles*. See http://noether.uoregon.edu/~sadofsky/634/Circle-wedge.pdf.

[27] J. Swiatkowski (2001), *Estimate for homological dimension of configuration spaces of graphs*. Colloquium Mathematicum, Volume 89, Page 69-79. Available at: http://www.math.uni.wroc.pl/~swiatkow/Papers/graf2.ps.

[28] Wikipedia, *Algorithms to find the number of path connected components of a graph*. Available at: http://en.wikipedia.org/wiki/Connected_component_(graph_theory)29#Algorithms.

[29] Wikipedia, *History of artificial intelligence*. Available at: `http://en.wikipedia.org/wiki/History_of_artificial_intelligence`.

[30] *History of robot*. Available at: `http://en.wikipedia.org/wiki/History_of_robots`.

[31] Wikipedia, *Unimate*. Available at: `http://en.wikipedia.org/wiki/Unimate`.

[32] Afra Zomorodian (2005), *Topology for Computing*. Content is available at: `http://www.cs.dartmouth.edu/~afra/book.html`.